LAMONT GEOLOGICAL OBSERVATORY
Columbia University
Palisades, New York

INTERNAL WAVES IN THE ARCTIC OCEAN

by

John Ross Yearsley

Technical Report No. 5
CU-5-66-Nonr 266 (82)

September 1966

LAMONT GEOLOGICAL OBSERVATORY
Columbia University
Palisades, New York

INTERNAL WAVES IN THE ARCTIC OCEAN

by

John Ross Yearsley

Technical Report No. 5

CU-5-66-Nonr 266 (82)

September 1966

TABLE OF CONTENTS

LIST OF FIGURES

NOMENCLATURE

(A partial list only)

$b_p^{(n)}$ - the n^{th} zero of the Bessel function of order p.

f - the Coriolis parameter $2\Omega \sin \varphi$.

k - the wave-number in the x-direction.

p - the total pressure associated with some particle of water, except where it occurs in: $b_p^{(n)}$, J_p, or N_p. In these three cases it refers to the order of the Bessel function.

p' - a small perturbation of pressure.

t - time.

u - the velocity in the direction of the x-axis.

v - the velocity in the direction of the y-axis.

w - the velocity in the direction of the z-axis.

x - a horizontal axis of the Cartesian coordinate system.

y - a horizontal axis of the Cartesian coordinate system along which there is no change in any variable.

z - the vertical axis of the Cartesian coordinate system aligned in the direction of decreasing gravity.

A - the ratio of the total density variation change to the maximum density.

J_p - the Bessel function of the first kind, of order p.

N_p - Weber's form of the Bessel function of the second kind, of order p.

α - an inverse length scale associated with the density distribution.

ζ - the vertical particle displacement.

ρ - the total density of a particle.

NOMENCLATURE

ρ_o - the time-average density.

τ - the time lag.

ϕ - the latitude, measured from the equator.

ω - the angular frequency of the free internal gravity waves.

Ω - the angular frequency of the Earth's rotation.

I. INTRODUCTION

1.1 Scope of the work.-- In recent years considerable attention has been given to the subject of internal waves. Much of the work has been of a theoretical nature, but it has become evident that more data from the open ocean is necessary to provide a basis for evaluating the theory and for indicating areas which require further analytical treatment. This work is concerned with both the theoretical and experimental aspects of internal waves in the Arctic Ocean.

The theoretical work is an investigation of free internal gravity waves in a rotating fluid. For a given vertical profile of the in situ density the theory leads to a description of the corresponding dispersion relation and eigenfunctions of the vertical amplitude. The mathematical model for the density profile used in this work gives a good approximation to the in situ density profile found in the Canadian Basin of the Arctic Ocean. With suitable changes in the parameters it could be used to model the density profile in other oceans or other fluids.

The experimental work is primarily a presentation of the power spectra of internal wave records. These records were obtained at depths of 60 and 125 meters during the summer of 1965. The limited extent of the experiment precludes any qualitative comparison between the data and the theory. However, the experimental results should be helpful in planning further studies in the Arctic and in providing knowledge of internal wave spectra as they occur in the real ocean.

1.2 Brief literature survey.-- Stokes(1849) has been credited with the first mathematical investigation of waves on the boundary between two fluids of different density. A number of authors subsequently elaborated upon this work, notably in extending the treatment to a fluid with a continuously-varying density profile.

Work by Ekman(1906) and Helland-Hansen and Nansen(1909) drew attention to the importance of internal waves in the ocean. During the early 1900's investigators made further attempts to learn about internal waves in the ocean, but it was Fjeldstad's(1933) analytical treatment of the subject which provided the basis for present work.

Since then there have been numerous papers, both of a theoretical and experimental nature, attempting to explain how internal waves are generated, how they propagate, and to determine the nature of the power spectrum. Notable theoretical papers dealing with the generation and propagation of internal waves have been those of Groen(1948), Haurwitz(1948, 1950), and Rattray(1957,1960). Important papers of an experimental nature have been published by Fjeldstad(1964), Haurwitz et al(1959), LaFond(1961), Lee(1961), and Reid(1962).

II. THEORY OF FREE INTERNAL GRAVITY WAVES IN THE ARCTIC OCEAN

2.1 Important assumptions.-- The following assumptions will be used in this work:

1. The fluid is incompressible and inviscid.
2. The motions are so small that second-order quantities can be neglected.
3. The density variations are important only where they are associated with the gravity term.
4. There is no variation of any parameter in the y-direction.
5. The density can be separated into two portions, a steady-state or average density denoted by a zero subscript, and a perturbation density denoted by a prime. That is:

$$\rho(x,y,z,t) = \rho_0(z) + \rho'(x,y,z,t)$$

6. The pressure can be separated into three portions, a constant term due to atmospheric pressure, a hydrostatic term due to an average density, and a perturbation term. That is:

$$p(x,y,z,t) = P_0 - \int_0^z \rho_0(z)\, g\, dz + p'(x,y,z,t)$$

7. The dynamical effects of the earth's sphericity can be ignored.
8. The only component of the angular velocity of the Earth which will be considered is the one opposite to that of gravity. This assumption is valid only for regions of high-latitude and mid-latitude.

2.2 Coordinate system.-- The Arctic Ocean will be approximated by an ocean of constant depth D, on a platform which is rotating at a constant angular frequency ω_0. The value of ω_0 is one-half the local Coriolis parameter $f=2\Omega\sin\Phi$, where Ω is the Earth's angular velocity of rotation and Φ is the latitude where the experiment was performed, measured from

the equator. The coordinate system will be the Cartesian coordinate system with the z-axis aligned in the direction opposite to that of gravity. Figure 1 shows the coordinate system.

2.3 Equations of motion.--Following the work of Fjeldstad (1933) the above assumptions and coordinate system lead to the following equations of motion:

$$\frac{\partial u}{\partial t} - fv = -\frac{1}{\rho_0}\frac{\partial p'}{\partial x} \qquad (2.3.1)$$

$$\frac{\partial v}{\partial t} + fu = 0 \qquad (2.3.2)$$

$$\frac{\partial w}{\partial t} = -\frac{1}{\rho_0}\frac{\partial p'}{\partial z} - \rho' g \qquad (2.3.3)$$

$$\frac{\partial u}{\partial x} + \frac{\partial v}{\partial y} + \frac{\partial w}{\partial z} = 0 \qquad (2.3.4)$$

$$\frac{\partial \rho'}{\partial t} + w\frac{d\rho_0}{dz} = 0 \qquad (2.3.5)$$

In the following work the vertical velocity w will be replaced by the vertical displacement ζ, by making use of the formula:

$$\frac{d\zeta}{dt} \cong \frac{\partial \zeta}{\partial t} = w \qquad (2.3.6)$$

2.4 The wave solutions.-- Since the depth over the entire basin has been assumed to be uniform and the variation in the y-direction has been assumed to be zero, a solution to the system of equations (2.3.1)-(2.3.5) can be found which has the form:

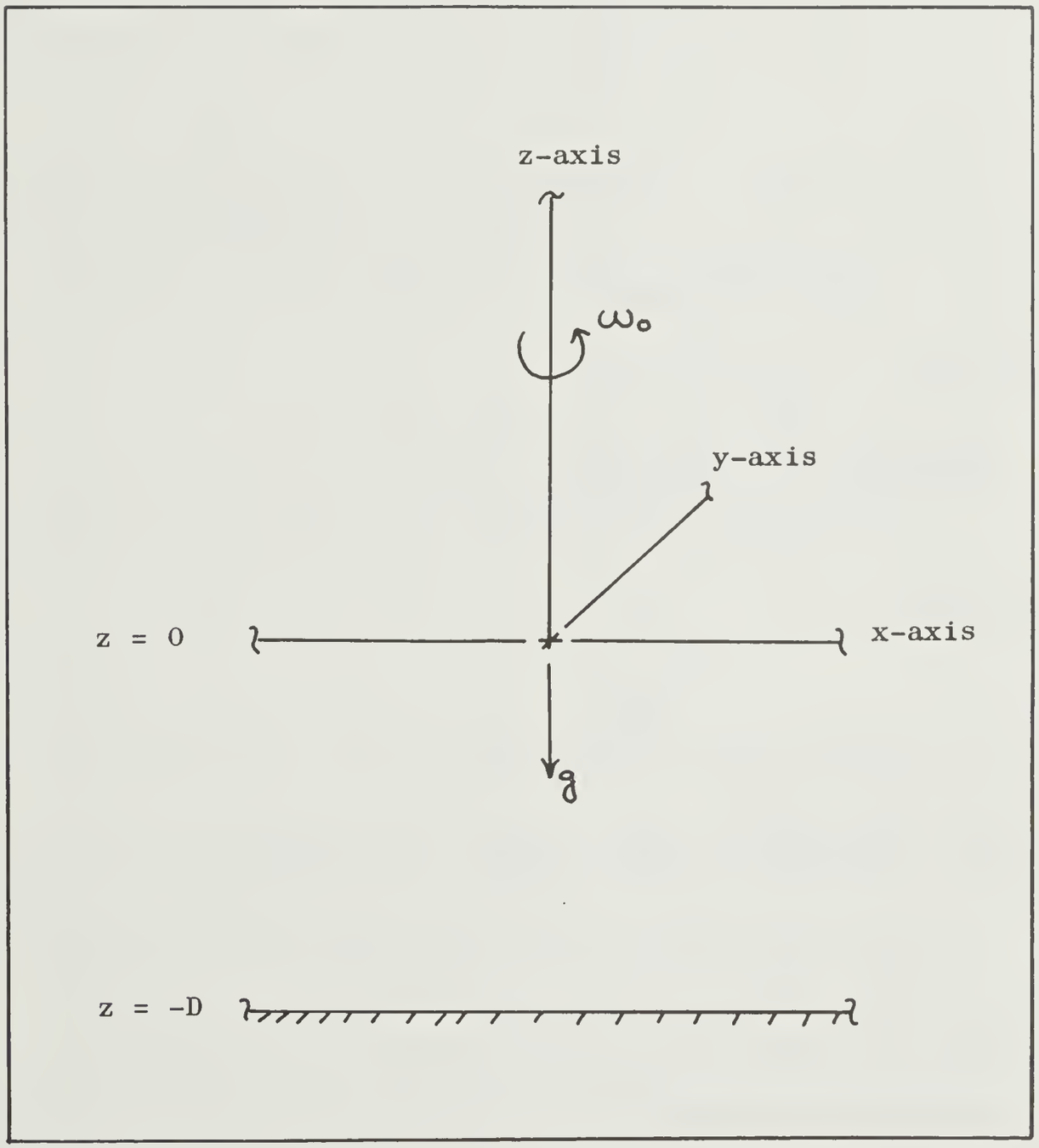

Figure 1. The coordinate system.

$$\left.\begin{aligned} u &= U(z) \\ v &= V(z) \\ \zeta &= \zeta(z) \\ p' &= \rho_0 \Pi(z) \\ \rho' &= \rho(z) \end{aligned}\right\} e^{i(kx + \omega t)} \qquad (2.4.1)$$

Substituting the values of the variables given in equation (2.4.1) into the equations (2.3.1)-(2.3.5) and eliminating all but the vertical displacement ζ leads to the following ordinary differential equation:

$$\frac{1}{\rho_0}\frac{d}{dz}\left[\rho_0 \frac{d\zeta}{dz}\right] - \left[\frac{g}{\rho_0}\frac{d\rho_0}{dz} + \omega^2\right]\left[\frac{k^2}{\omega^2 - f^2}\right]\zeta = 0 \qquad (2.4.2)$$

A more convenient form of the equation is obtained by the substitution:

$$\zeta = \frac{\eta}{\sqrt{\rho_0}} \qquad (2.4.3)$$

which results in the equation:

$$\frac{d^2\eta}{dz^2} + \left\{\frac{1}{4}\left[\frac{1}{\rho_0}\frac{d\rho_0}{dz}\right]^2 - \frac{1}{2\rho_0}\frac{d^2\rho_0}{dz^2} - \left[\frac{g}{\rho_0}\frac{d\rho_0}{dz} + \omega^2\right]\left[\frac{k^2}{\omega^2 - f^2}\right]\right\}\eta = 0 \qquad (2.4.4)$$

In the Arctic Ocean, as in most oceans, the first two terms in the brackets of equation (2.4.4) can be neglected (see Appendix I). A general solution to (2.4.4) can then be obtained if the form of the average density distribution $\frac{d\rho_0}{dz}$ is specified. Numerous models for this density distribution have been investigated. A particular model which has not been investigated and gives a close approximation to the actual <u>in situ</u> density distribution in the Arctic Ocean

is the following:

$$\rho_o(z) = \rho_o(-D)\left[1 - A e^{\alpha z}\right] \qquad (2.4.5)$$

Substituting this into equation (2.4.4) gives:

$$\frac{d^2\eta}{dz^2} + \left[\beta e^{\alpha z} - \varkappa^2\right]\eta = 0 \qquad (2.4.6)$$

where $\beta = \alpha A g\left[\frac{k^2}{\omega^2 - f^2}\right]$ and $\varkappa^2 = \frac{\omega^2 k^2}{\omega^2 - f^2}$.

Equation (2.4.6) reduces to Bessel's equation:

$$r^2 \frac{d^2 m}{dr^2} + r \frac{dm}{dr} + \left(r^2 - p^2\right) m = 0 \qquad (2.4.7)$$

by the substitution $\eta(z) = m(r)$, where $\alpha r = 2\sqrt{\beta}\, e^{\alpha z/2}$ and $p^2 = \frac{4\varkappa^2}{\alpha^2}$.

The general solution of equation (2.4.7) is then:

$$m(r) = C J_p(r) + D N_p(r) \qquad (2.4.8a)$$

or,

$$\eta(z) = \sqrt{\rho_o}\,\zeta(z) = C J_p\left(\frac{2\sqrt{\beta}}{\alpha} e^{\frac{\alpha z}{2}}\right) + D N_p\left(\frac{2\sqrt{\beta}}{\alpha} e^{\frac{\alpha z}{2}}\right) \qquad (2.4.8b)$$

2.5 Boundary conditions.-- To specify the problem completely, boundary conditions are needed. Most theoretical analyses of wave motion in the deep ocean require that the surface ($z = 0$) pressure be continuous with the atmospheric pressure. However, the pack ice covering the Arctic Ocean acts like a lid, particularly for the shorter period waves, as Hunkins (1962) has shown. This means that the dynamic boundary condition at the surface can be replaced by a kinematic boundary condition requiring no vertical motion at the surface. For the very long waves in the deep ocean the pack ice is not such

an effective lid, but the amplitudes of the vertical motion at the surface are so small compared to the wave-length that the dynamic boundary condition and the kinematic boundary condition are very nearly equivalent.

The boundary condition at the bottom(z = -D) requires that the particle displacement there be zero.

Symbollically, the above arguments can be stated as:

$$\varsigma = 0, \text{ at } z = 0 \qquad (2.5.1)$$

$$\varsigma = 0, \text{ at } z = -D \qquad (2.5.2)$$

2.6 The eigen-values.-- With the above boundary conditions the eigen-values are determined by finding the roots of the equation:

$$J_p\left(\frac{2\sqrt{\beta_n}}{\alpha}\right) N_p\left(\frac{2\sqrt{\beta_n}}{\alpha} e^{-\frac{\alpha D}{2}}\right) - J_p\left(\frac{2\sqrt{\beta_n}}{\alpha} e^{-\frac{\alpha D}{2}}\right) N_p\left(\frac{2\sqrt{\beta_n}}{\alpha}\right) = 0 \qquad (2.6.1)$$

Writing equation (2.6.1) in the form:

$$J_p(b_n) N_p(\gamma b_n) - J_p(\gamma b_n) N_p(b_n) = 0 \qquad (2.6.2)$$

where $\gamma = e^{-\frac{\alpha D}{2}}$ and $b_n = \frac{2\sqrt{\beta_n}}{\alpha}$ it can be shown tha the roots of this equation approach the roots of:

$$J_p(b) = 0 \qquad (2.6.3)$$

as $\gamma \to 0$. A demonstration of this is found in Kline(1948), who shows in the same paper that the roots of equation (2.6.2) are unique and positive as $\gamma \to 0$, and that the correspondence between the roots of equations (2.6.2) and (2.6.3) is one-to-one.

To determine the error in replacing equation (2.6.2) by (2.6.3) consider a depth D of 3000 meters, which is typical for the Canadian Basin, and a value of α equal to 0.8×10^{-2} meters^{-1}, then γ is about 10^{-5}. The most slowly converging root of (2.6.2) is the first root of zero order (according to figure 1 (page 34) of Kline(1948).) According to the same reference the error which results from replacing equation (2.6.2) by (2.6.3) for $\gamma = 10^{-5}$ is of the order of one part in 10^4, for the first root of the zero order. The error for all other roots would be less than this.

Since the maximum error for the conditions in the Arctic Ocean is so small it is reasonable to use equation (2.6.3) to determine the eigen-values. By determining the values of the constants in equation (2.4.5) it is possible to describe the dispersion relation by making use of equation (2.6.3). As can be seen from figure 2, the following values substituted into equation (2.4.5) give a close approximation to the actual <u>in situ</u> density distribution of the Arctic Ocean:

$$\begin{aligned} \alpha &= 0.8 \times 10^{-2} \text{ meters}^{-1} \\ A &= 5.0 \times 10^{-3} \\ \rho_o(-D) &= 1.028 \text{ grams/cc.} \end{aligned} \qquad (2.6.4)$$

If $b_n^{(p)}$ is the n^{th} root of equation (2.6.3) then:

$$b_n^{(p)} = \frac{2\sqrt{\beta_n}}{\alpha} \qquad (2.6.5)$$

Substituting the necessary values of the constants from equation (2.6.4) into the definition of β given previously

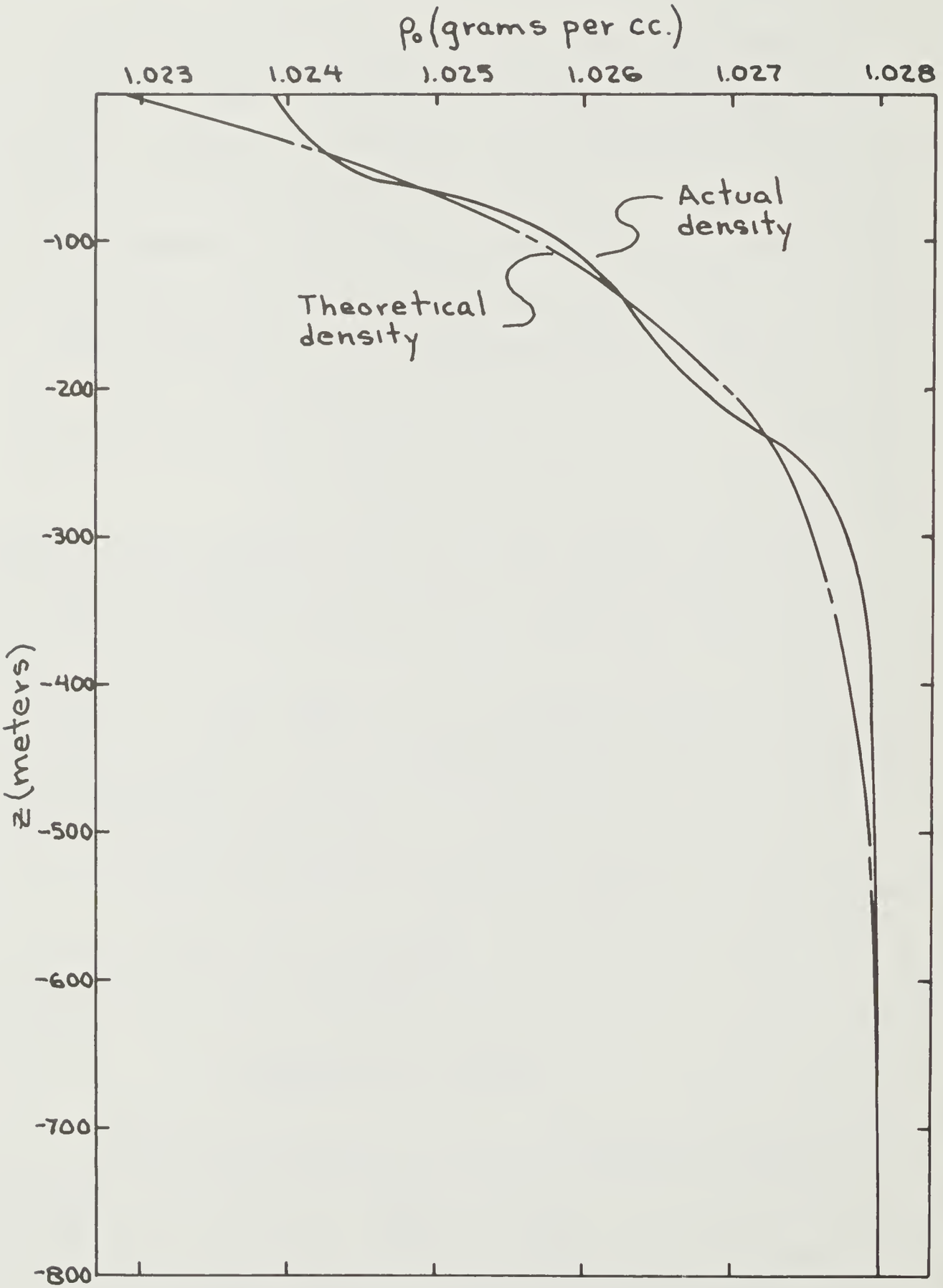

Figure 2. The in situ density profile.

and making use of the same definition in equation (2.6.5) leads to the following dispersion relation:

$$\omega_n^2 = f^2 + \frac{25\, k_n^2}{[b_n^{(p)}]^2} \qquad (2.6.6)$$

where ω_n and f are expressed in radians/sec. and k_n in meters^{-1}, and, as before, $p^2 = \frac{4\pi^2}{\alpha^2}$.

Figures 3,4,5, and 6 show, respectively, the first three modes of $\Im_W/Cn$ for the angular frequencies $1.4\text{x}10^{-4}$ radians/sec., $2.0\text{x}10^{-3}$ radians/sec., and $1.1\text{x}10^{-2}$ radians/sec., and the dispersion relation, equation (2.6.6).

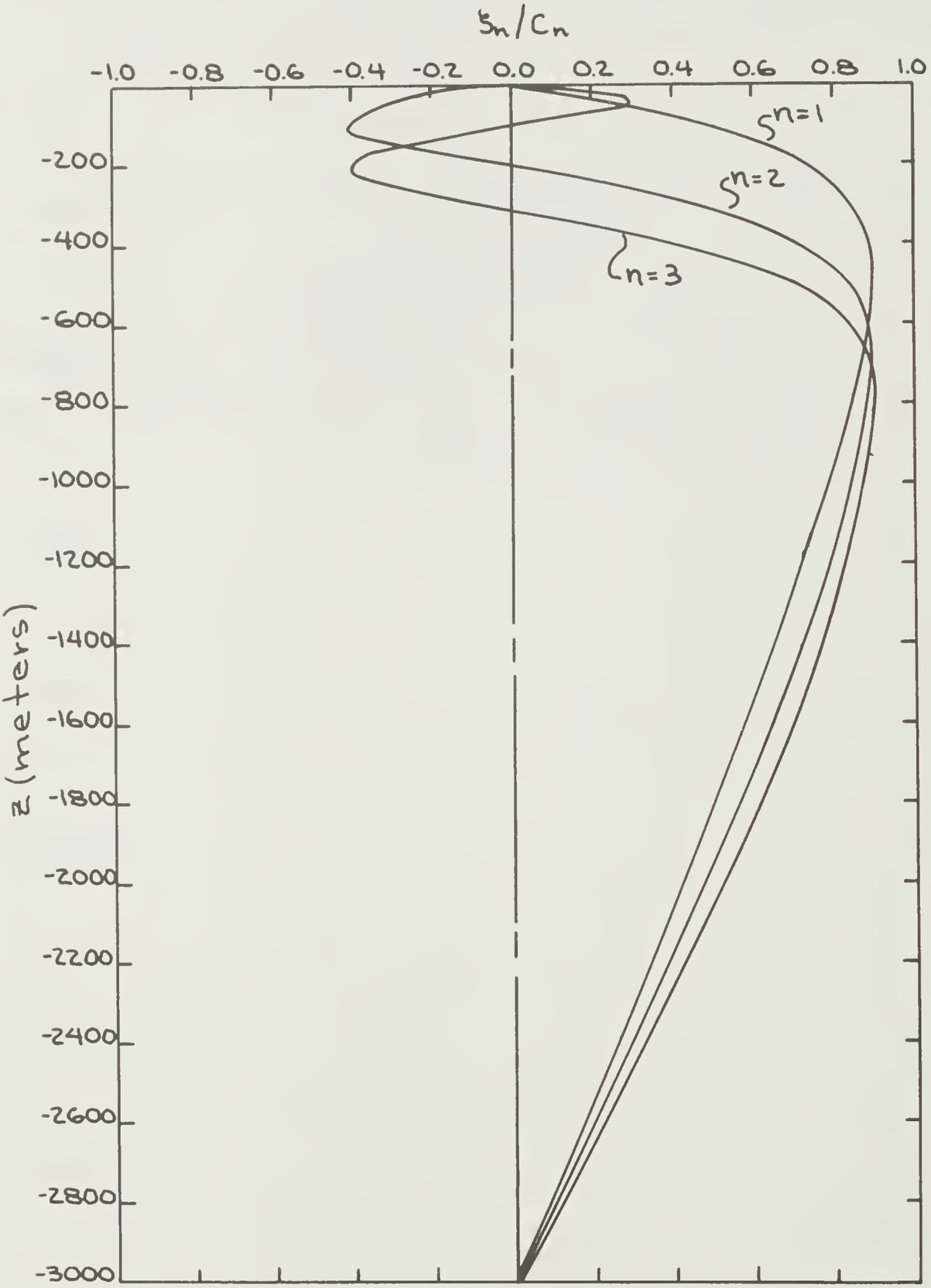

Figure 3. ζ_n/C_n for $n=1,2,3$ and $\omega = 1.40 \times 10^{-4}$ radians per second.

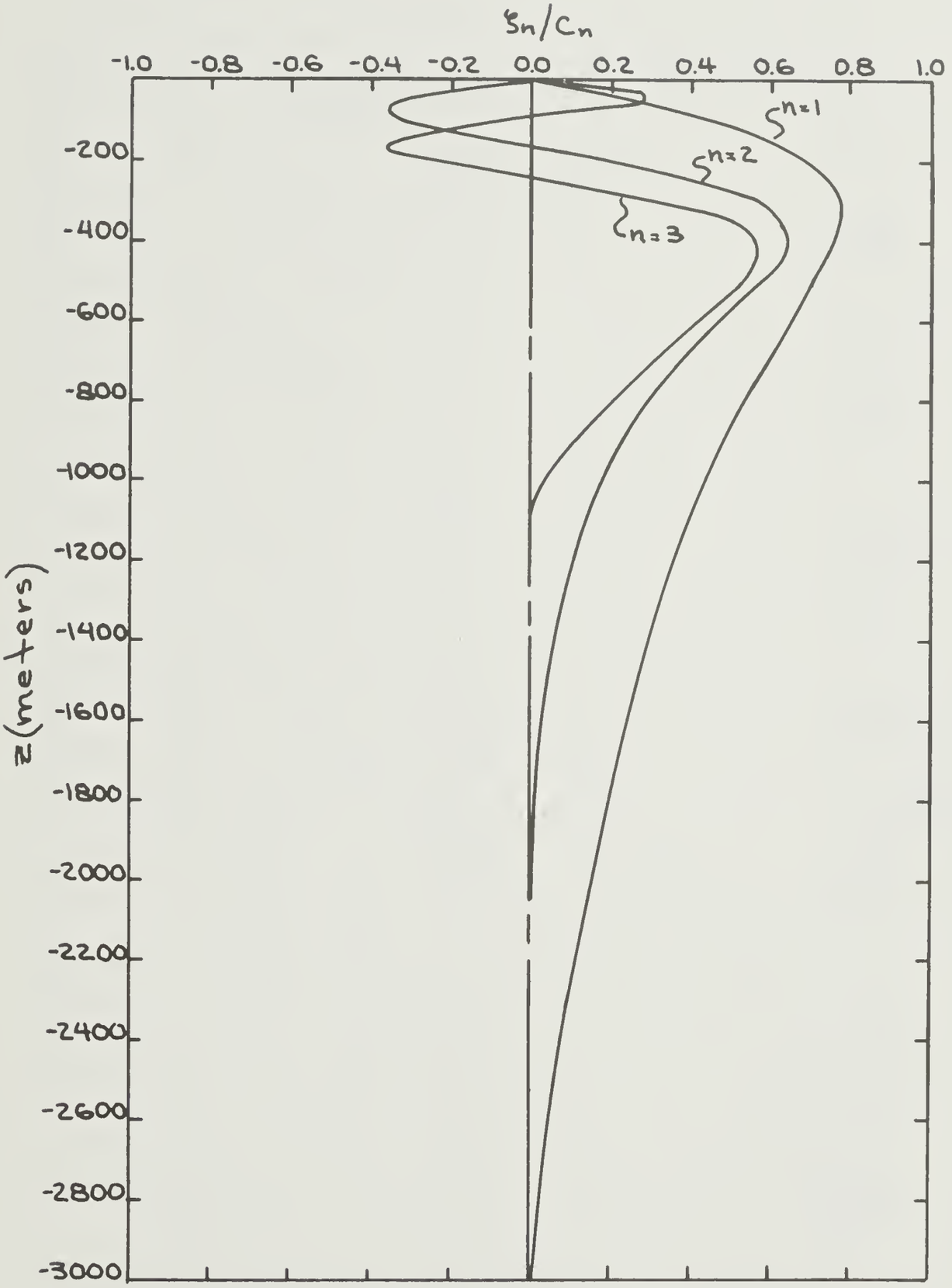

Figure 4. ζ_n/C_n for $n=1,2,3$ and $\omega = 2.00 \times 10^{-3}$ radians per second.

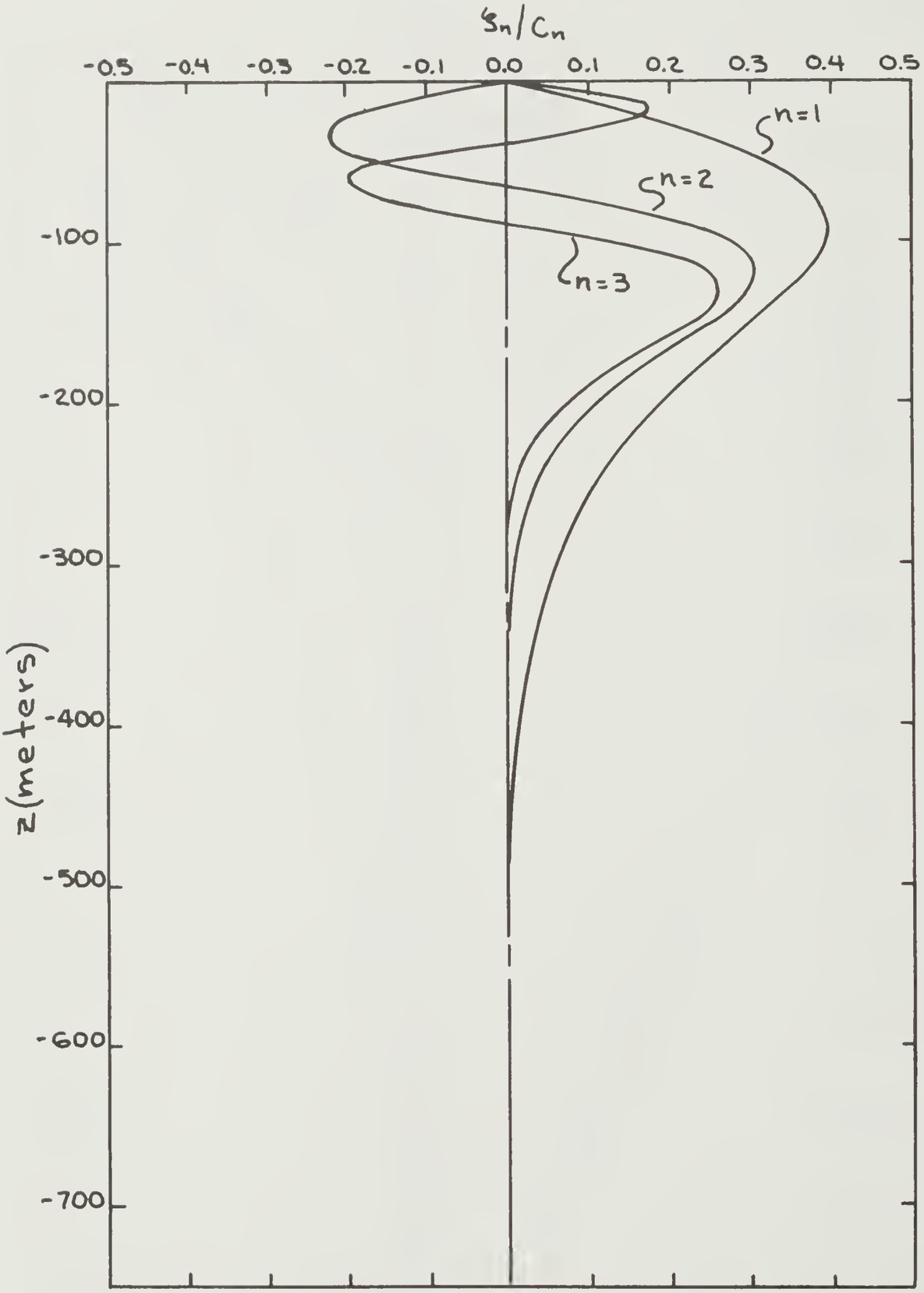

Figure 5. ζ_n/C_n for n= 1,2,3 and $\omega = 1.05 \times 10^{-2}$ radians per second.

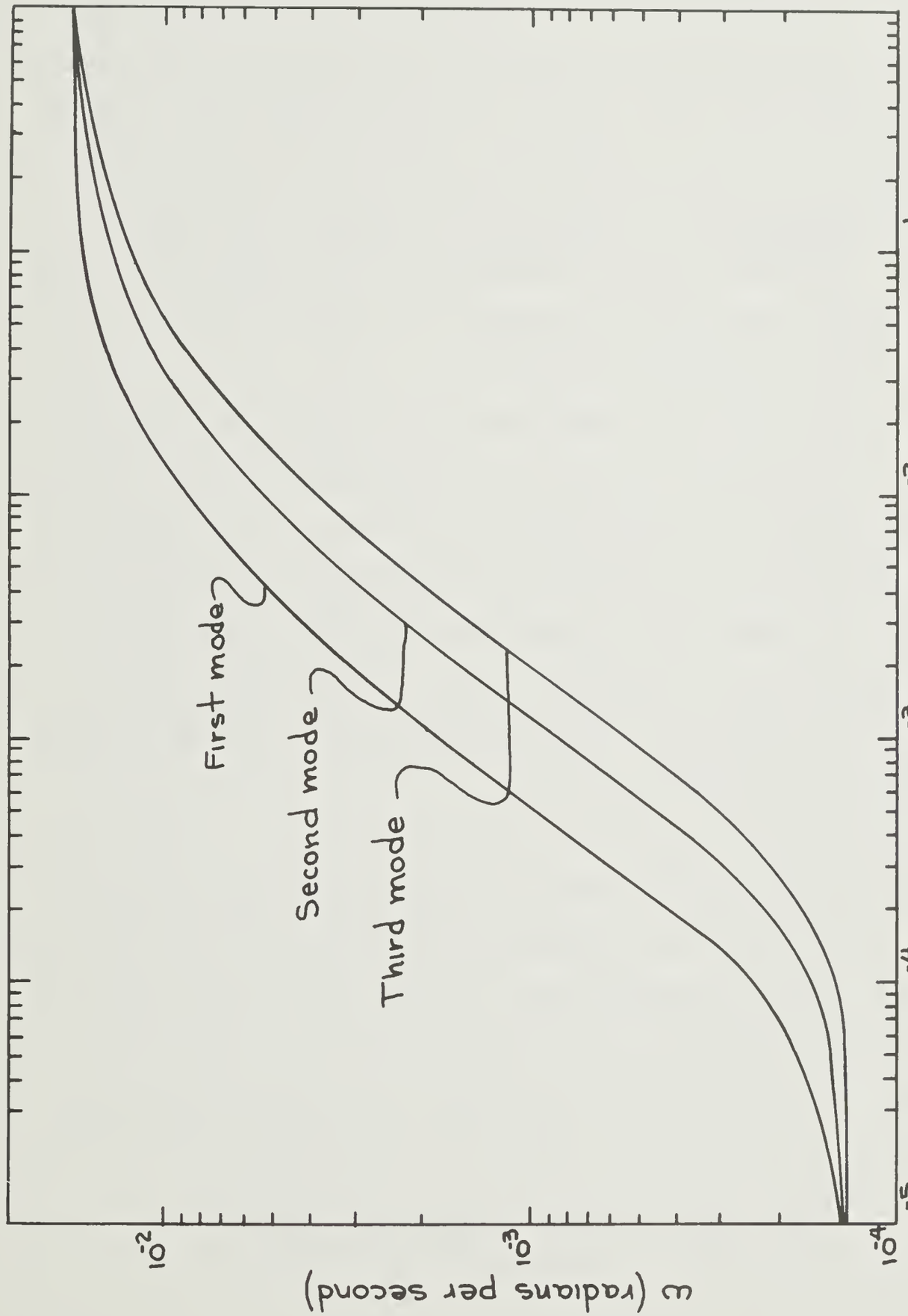

Figure 6. Dispersion relation for the first three modes.

III. EXPERIMENTAL WORK

3.1 Development of the experiment.-- With the exception of the work by Haurwitz et al(1959) measurements of internal waves in the real ocean have been obtained from stations located along the continental shelf rather than in the deep ocean. In an attempt to add to the information from deep ocean stations an experiment was conducted on ice island T-3 during the summer of 1965. The ice island was in the Canadian Basin of the Arctic Ocean and its position at important times during the summer are given in table 1.

The Arctic Ocean was chosen for the experiment for a number of reasons. (1) The ice island provides a very stable platform from which to conduct an investigation of waves. (2) The horizontal gradients of temperature and salinity are small. (3) There are no swift currents which might affect the propagation of internal waves. (5) The density distribution is such that it can be modeled quite well by a simple mathematical expression.

The primary purpose of the experiment was to determine the power spectrum of internal waves at various depths.

To determine the amplitude of the internal waves the procedure has been in most cases to determine the variation of some depth-dependent conservative property as a function of time. That is, if $\Theta(x,y,z,t)$ is a conservative property, then:

$$\frac{d\Theta}{dt} = \frac{\partial\Theta}{\partial t} + u\frac{\partial\Theta}{\partial x} + v\frac{\partial\Theta}{\partial y} + w\frac{\partial\Theta}{\partial z} = 0 \qquad (3.1.1)$$

Table 1. Positions of T-3.

DATE	TIME*	LATITUDE	LONGITUDE
[1]7/20/65	1200Z	76° 07.6' N.	141° 59' W.
[2]8/10/65	2000Z	75° 30.5' N.	140° 16' W.
[3]8/24/65	2015Z	75° 57.0' N.	139° 38' W.
9/ 6/65	2200Z	75° 24.3' N.	139° 51' W.
9/10/65	0130Z	75° 22.8' N.	140° 10' W.
9/10/65	0800Z	75° 21.5' N.	140° 12' W.
9/11/65	0600Z	75° 21.0' N.	140° 15' W.
9/12/65	0630Z	75° 22.2' N.	140° 15' W.
9/13/65	0730Z	75° 23.4' N.	140° 14' W.

[1]Date on which hydrographic station 1-65 was made.

[2]Date on which hydrographic station 2-65 was made.

[3]Date on which hydrographic station 3-65 was made.

*Z indicates Greenwich Mean Time.

This property can be considered as being composed of a time-average component $\Theta_0(x,y,z)$ and a small perturbation component $\Theta'(x,y,z,t)$. If the time-average component has large characteristic lengths in the horizontal then equation (3.1.1) can be written approximately as:

$$\frac{\partial \Theta'}{\partial t} + \frac{\partial \zeta}{\partial t} \frac{d\Theta_0}{dz} = 0 \qquad (3.1.2)$$

Integrating this equation leads to the result:

$$\zeta(x,y,z,t) = - \frac{\Theta'(x,y,z,t)}{\frac{d\Theta_0}{dz}} \qquad (3.1.3)$$

from which the amplitudes for the spectral analysis can be determined.

In the Arctic Ocean one of the variables which satisfies the above requirements is the in situ temperature. It is also true that the instrumentation required to measure in situ temperature is much less complex, more stable and more accurate than that required to measure other conservative properties such as salinity or in situ density.

3.2 Instrumentation.-- The sensors used to determine the vertical displacements were Fenwal thermistors (type GB32P28) mounted in plastic tubes with a potting compound (Scotch Cast) to protect the joint where the thermistor was soldered to the marine connector.

The thermistor was attached to the end of a two-conductor armored cable. A bight was taken in the cable and a 40-pound lead weight was attached. Two cables with thermistors attached in this manner were lowered through a hole in the

pack ice near the edge of the island. The lines were measured at the surface and marked so that one thermistor would be located at a depth of 125 meters and the other at a depth of 60 meters. A pressure transducer was connected to the end of the 125-meter cable to monitor depth variations caused by changes in the wire angle. The 60-meter cable was lashed to the 125-meter cable so that any variations in the depth of the 60-meter cable could be detected by the pressure transducer. The final positioning of the equipment is shown schematically in figure 7.

From the hole in the pack ice the leads went to an equipment shack on the island, about 75 meters from the hole. Inside the shack was the recording equipment which consisted of an unbalanced Wheatstone bridge, a Varian G-10 amplifier and a large cylindrical drum upon which the recording paper was placed. An ink pen driven by the amplifier recorded the output on the paper strapped to the drum. The drum revolved at the rate of one revolution per hour and translated at about four centimeters per hour. At these speeds each sheet of paper produced a record approximately 12 hours in length. Figure 8 is a schematic diagram of the recording equipment.

The motor driving the drum was of the synchronous type, and since the power provided by the camp generator varied between 57 and 62 cycles per second it was necessary to use a time mark provided by a precision chronometer. The chronometer was insensitive to both voltage and frequency changes.

At the end of each 12-hour record the thermistor was

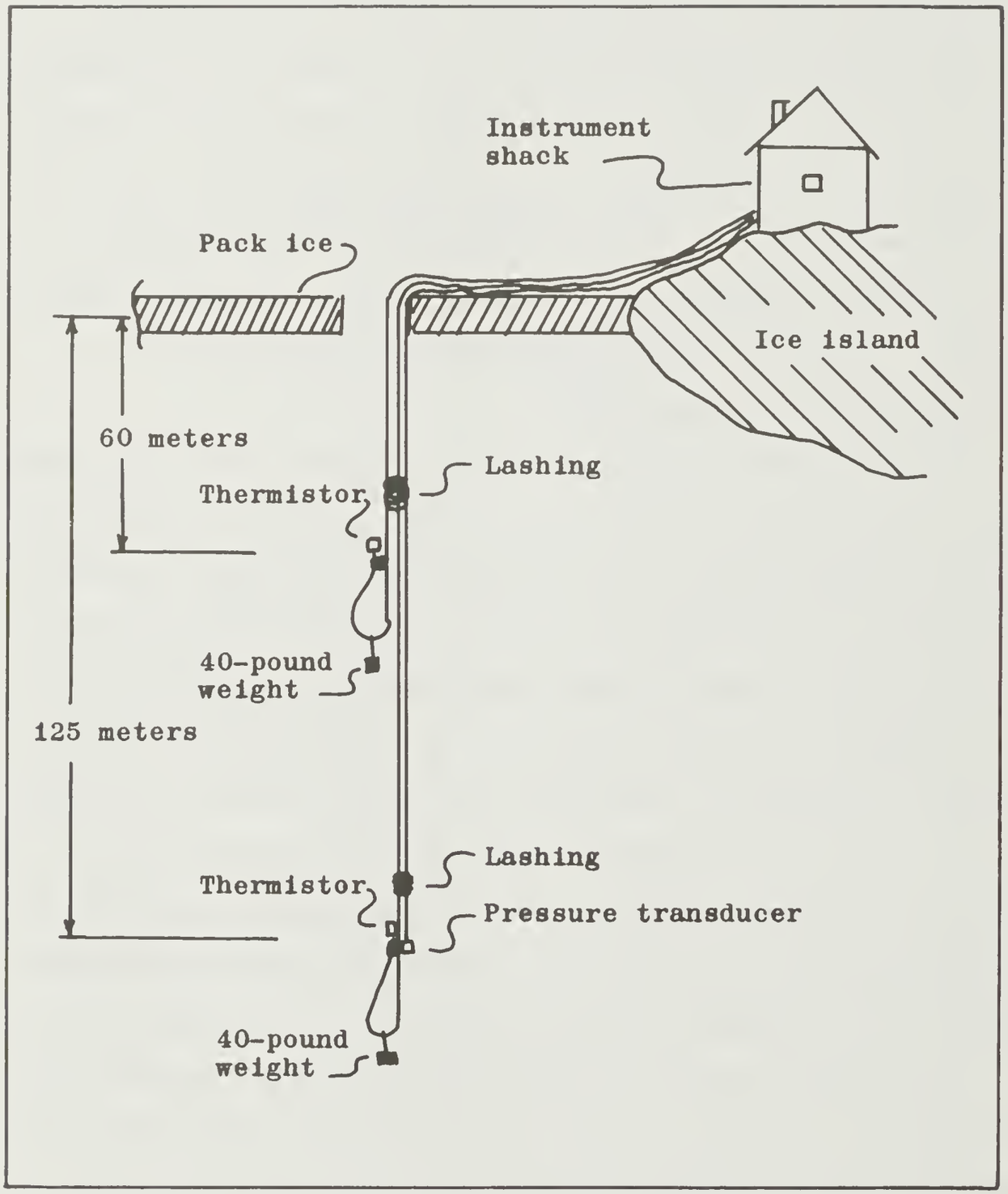

Figure 7. Schematic diagram of thermistor array.

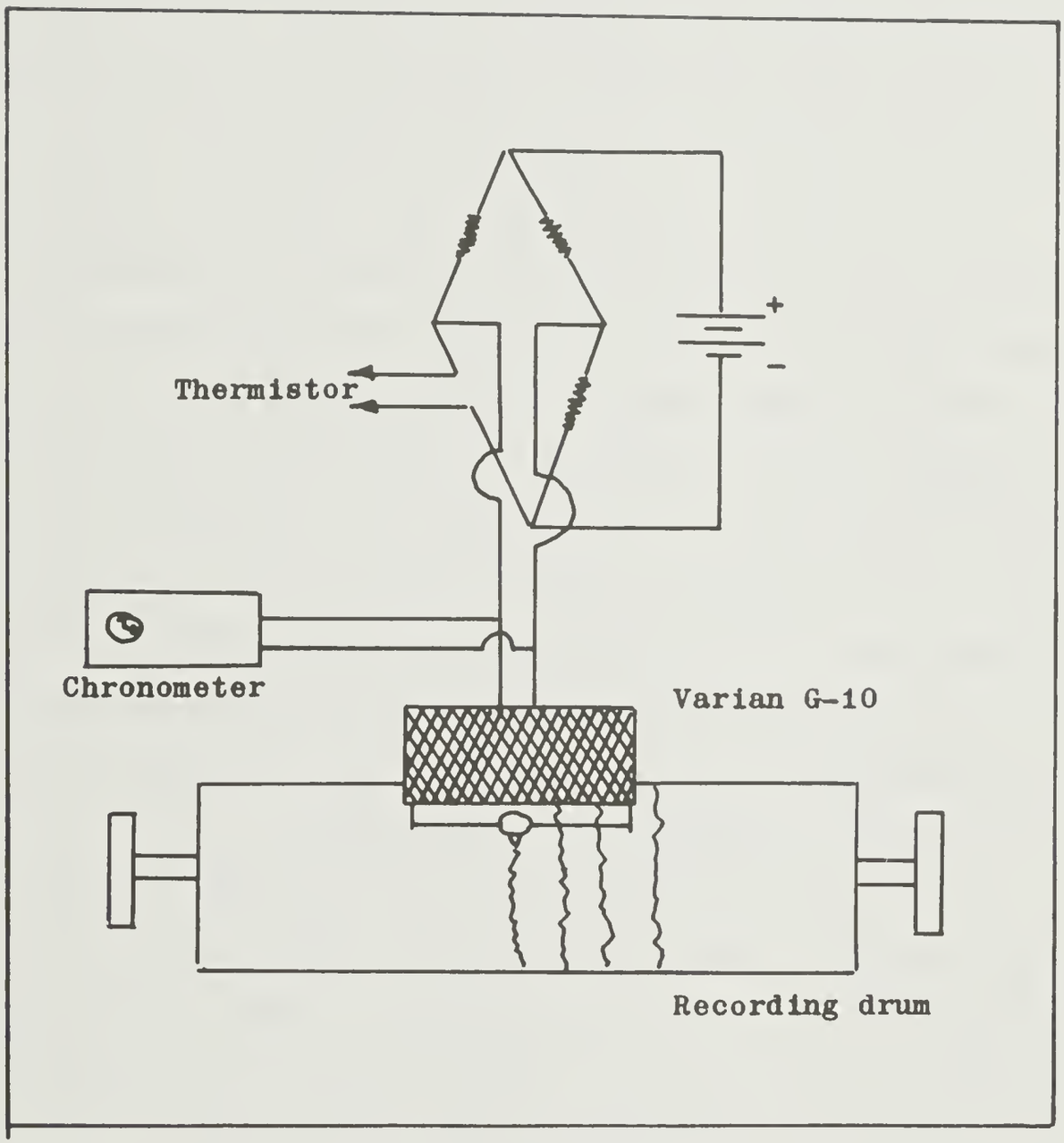

Figure 8. Schematic diagram of recording equipment.

removed from the bridge and replaced by a high-precision decade resistance box. By varying the resistance of the decade box a calibration curve was obtained for each record.

The output from the pressure transducer was recorded on a Rustrak recorder provided by the manufacturer of the transducer. The chart was calibrated in meters. Two scales were provided, an absolute scale which gave the actual depth and could be read to an accuracy of $\pm$2 meters, and an expanded scale which measured the variations from some nominal depth. The expanded scale could be read to an accuracy of $\pm$.4 meters.

3.4 Data.-- The portion of the experiment with which this work is concerned covered the period from 0725Z September 8, 1965 to 2305Z September 12,1965. This period was chosen because the low relative velocity between island and ocean at the time produced no observable wire angle, according to pressure transducer data. This was also the longest period for which all the equipment worked properly.

It was not possible to make determinations of hydrographic conditions during this period due to a malfunction of the salinometer. It was therefore necessary to assume that data obtained from hydrographic stations made a few weeks earlier would provide sufficient knowledge of conditions at the time of the experiment. This assumption was justified by the fact that the island moved very little between the time of the first hydrographic station and the end of the experimental section under consideration (see table 1). It is also well known from the work of such investigators as Coachman(1963)

and Worthington (1953) that the horizontal gradients of temperature and salinity in this region are very small. This is further emphasized by the fact that the three stations used in this work (see figure 9) show very little difference in values of temperature and salinity as a function of depth, even though they span a period of several weeks.

3.5 Reduction of the data.-- The resistance of the thermistor as a function of time was determined from the record by making use of the calibration points at the end of each record and time marks provided by the precision chronometer. The zero line, or null point, for each record was also obtained from the time mark. This was possible because the time mark was produced by shorting the input to the G-10 amplifier (see figure 8) at exactly one-minute intervals.

The temperature gradient with respect to thermistor resistance, $\frac{dT_o}{dR_o}$, was obtained from the calibration curve for each thermistor, and the temperature gradient with respect to depth, $\frac{dT_o}{dz}$, from the hydrographic stations. The particle displacement as a function of time and space was then determined from the equation:

$$\zeta(x,y,z,t) = -\frac{R'(x,y,z,t)}{\frac{dR_o}{dz}} \qquad (3.5.1)$$

where $R'(x,y,z,t)$ are the perturbations in thermistor resistance obtained from the record, and $\frac{dR_o}{dz} = \frac{1}{\frac{dT_o}{dR_o}} \times \frac{dT_o}{dz}$.

The raw data was smoothed by eye such that variations of periods less than two minutes were eliminated. The records could be read to an accuracy of ± 1 ohm. In terms of particle

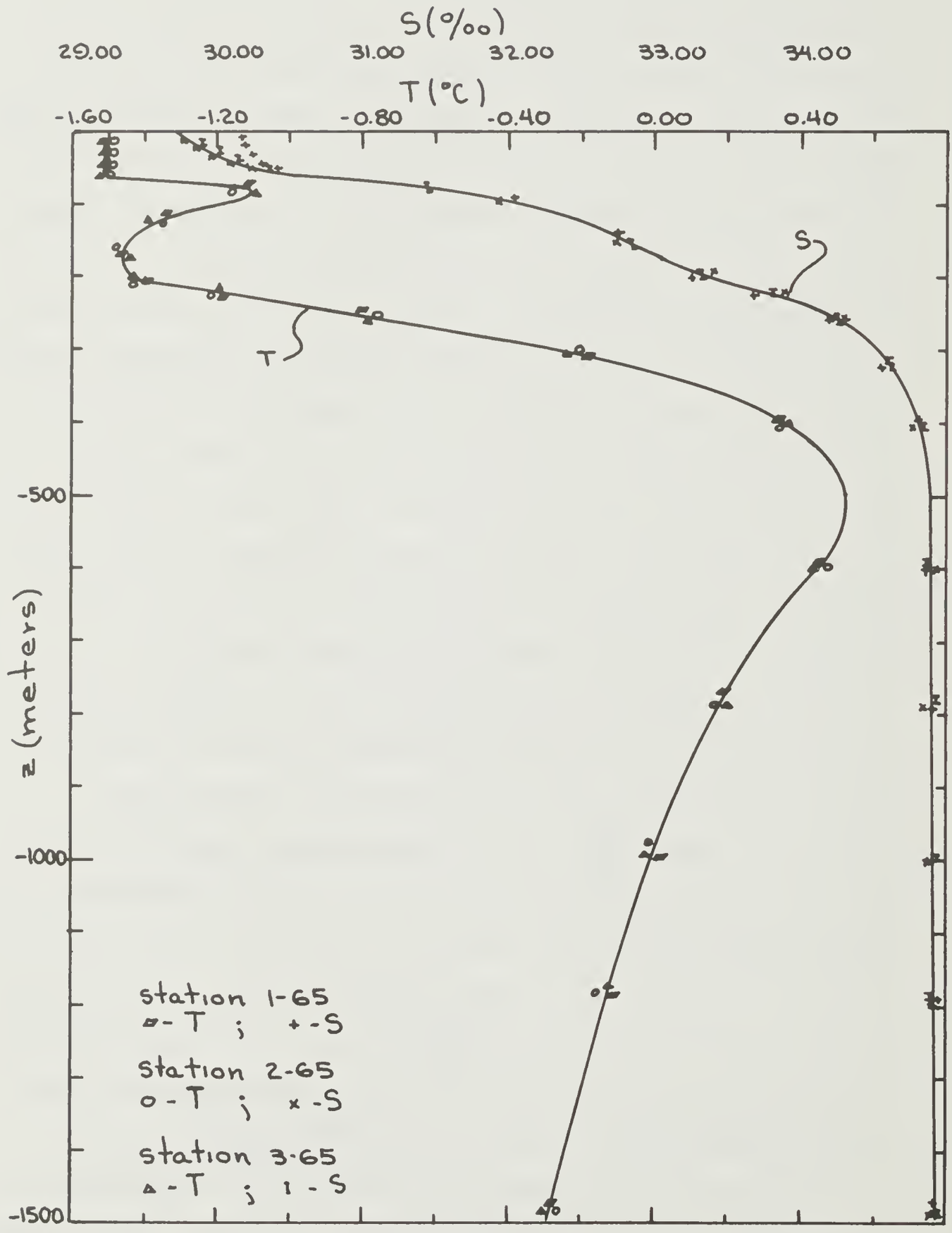

Figure 9. Temperature and salinity as a function of depth.

displacement this would correspond to ±13 centimeters for the 60-meter record and ±52 centimeters for the 125-meter record.

Figures 10 through 27 are copies of the original data.

3.6 Method of analysis.-- Analysis of the data was accomplished using methods described in Blackman and Tukey(1958).

For a function of time X(t) generated by a random process the autocorrelation function $R_x(\tau)$ is given by:

$$R_x(\tau) = \lim_{T \to \infty} \left\{ \frac{1}{T} \int_0^T X(\tau) \cdot X(t+\tau)\, dt \right\} \qquad (3.6.1)$$

The Fourier cosine transform of (3.6.1) determines the power spectrum $P_x(\omega)$:

$$P_x(\omega) = \frac{2}{\pi} \int_0^\infty R_x(\tau) \cos(\omega\tau)\, d\tau \qquad (3.6.2)$$

When the data points are obtained at finite intervals the power spectrum is determined by numerical integration of equations (3.6.1) and (3.6.2). The estimate of the autocorrelation function is:

$$R_x(l\Delta t) = \frac{1}{n_o - l} \sum_{q=1}^{n_o - l} X_q \cdot X_{q+l} \quad ; \; l = 0, 1, 2, \cdots S \qquad (3.6.3)$$

where n_o is the total number of data points and $s\Delta t$ determines the maximum lag τ. The raw estimate of the power spectrum is given by:

$$P_x(\omega_h) = P\left(\frac{h\pi}{s\Delta t}\right) = \frac{2\Delta t}{\pi} \sum_{l=0}^{S} \epsilon_l R_x(l\Delta t) \cos\left(\frac{hl\pi}{s}\right); \; h = 0, 1, \cdots S \qquad (3.6.4)$$

where $\epsilon_l = \begin{cases} 1 & 0 < l < s \\ 1/2 & l = 0, s \end{cases}$.

Since the record is of finite length, only estimates of smoothed values of the true spectral density can be found.

This is accomplished by smoothing the raw estimates by the "hamming" method described in Blackman and Tukey(1958):

$$SP_x^{(0)} = .54\,P_x^{(0)} + .46\,P_x^{(1)} \qquad (3.6.5a)$$

$$SP_x^{(k)} = .23\,P_x^{(k-1)} + .54\,P_x^{(k)} + .23\,P_x^{(k+1)} \qquad (3.6.5b)$$

$$SP_x^{(s)} = .46\,P_x^{(s-1)} + .54\,P_x^{(s)} \qquad (3.6.5c)$$

Estimates of the power spectra were calculated on an IBM 7094 using a program incorporating the above principles. The program was made available by M. Rona of the University of Washington's Computer Center.

Figures 28 through 45 are estimates of the power spectrum for each record.

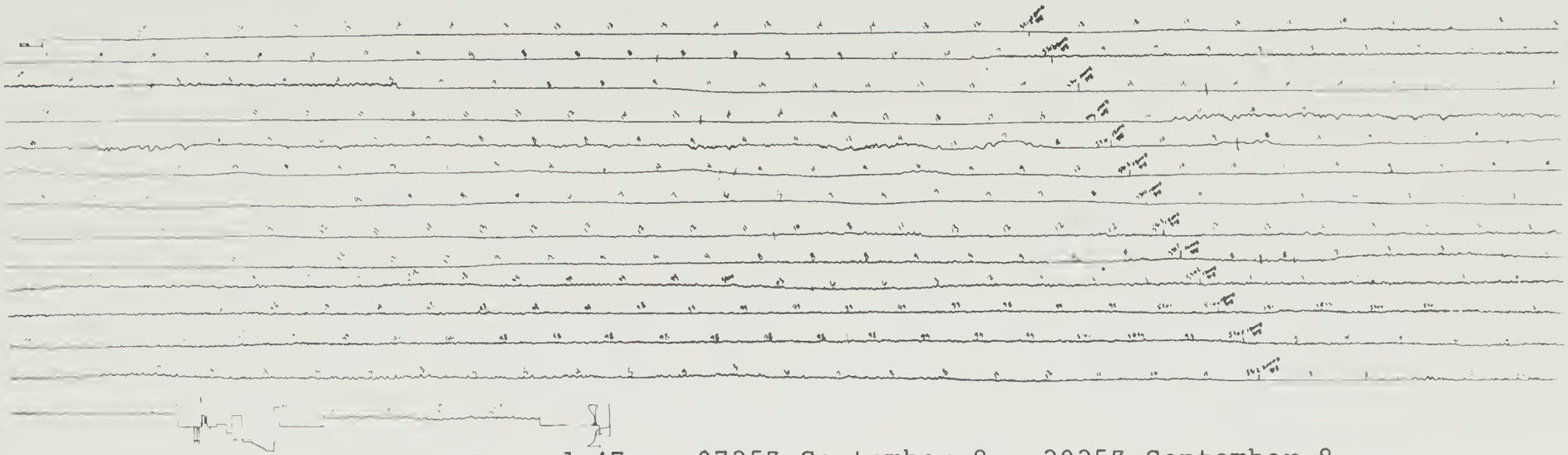

Figure 10. Record 47c. 0725Z September 8 - 2025Z September 8.
Thermistor depth - 60 meters.

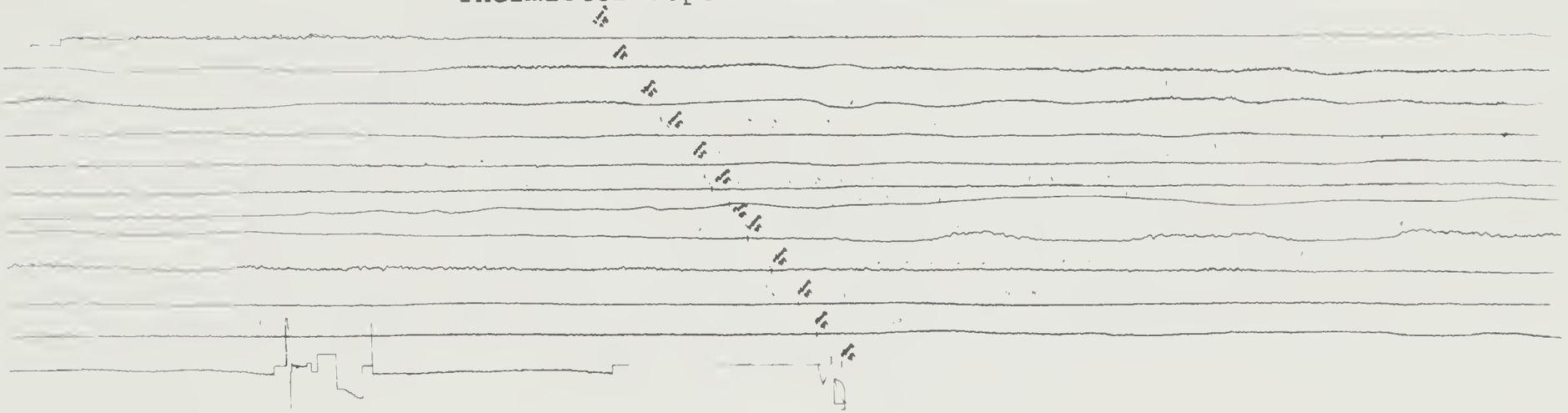

Figure 11. Record 48c. 2040Z September 8 - 0800Z September 9.
Thermistor depth - 60 meters.

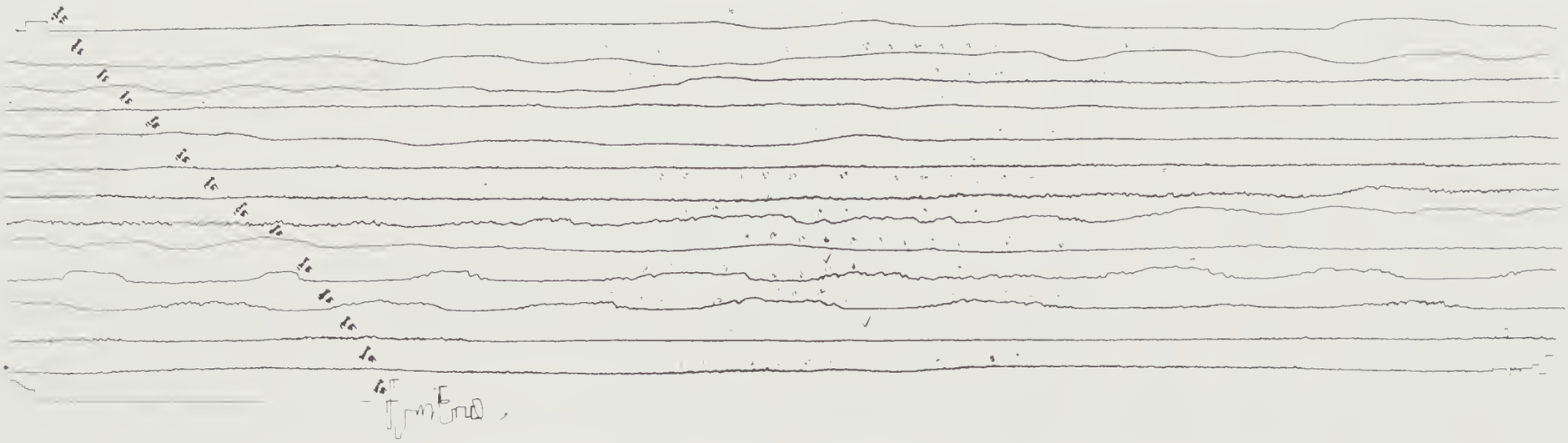

Figure 12. Record 49c. 0800Z September 9 - 2100Z September 9.
Thermistor depth - 60 meters.

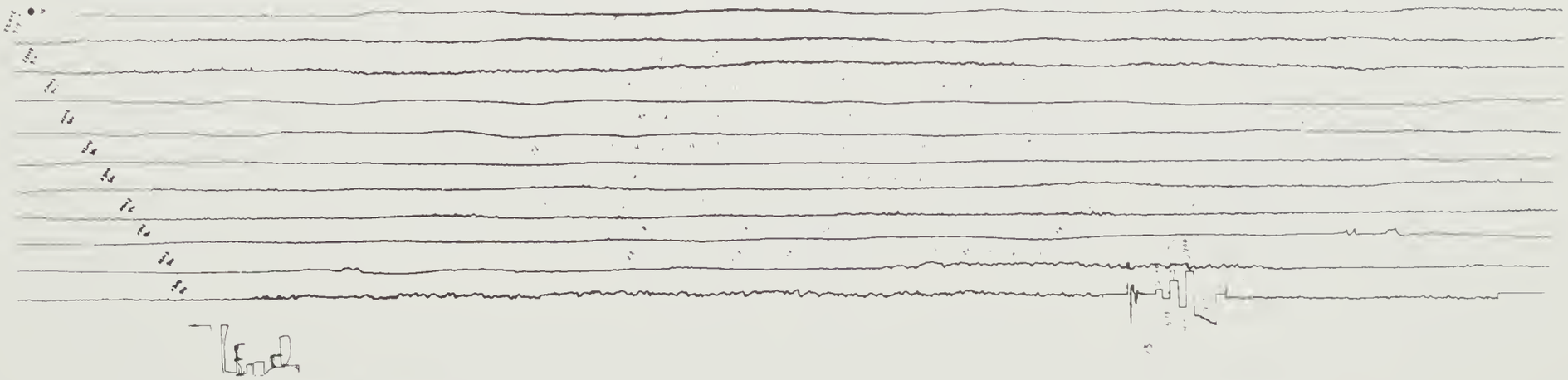

Figure 13. Record 50c. 2100Z September 9 - 0730Z September 10.
Thermistor depth - 60 meters.

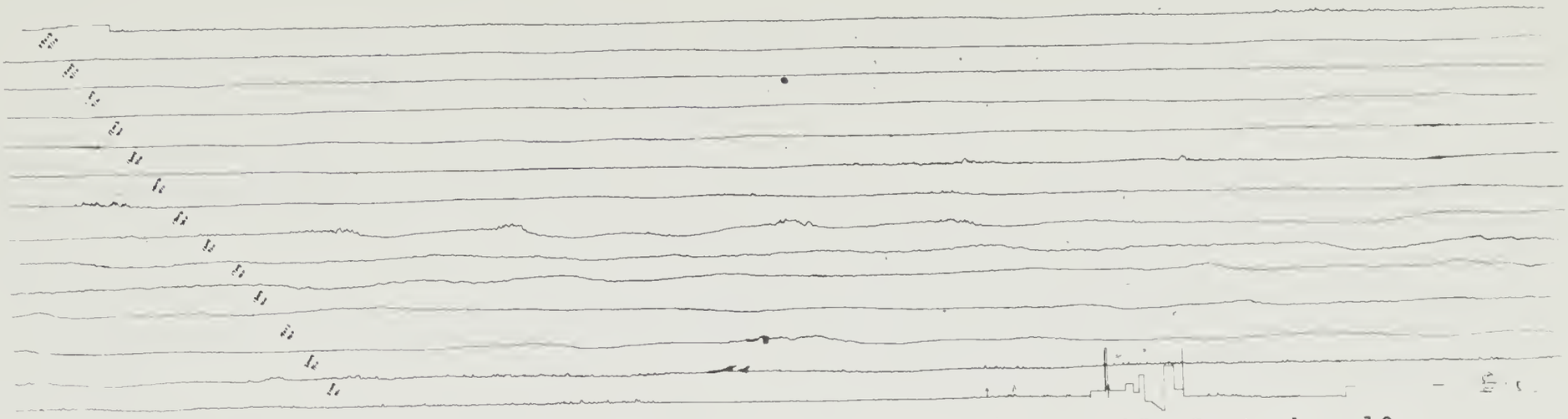

Figure 14. Record 51c. 0805Z September 10 - 2115Z September 10. Thermistor depth - 60 meters.

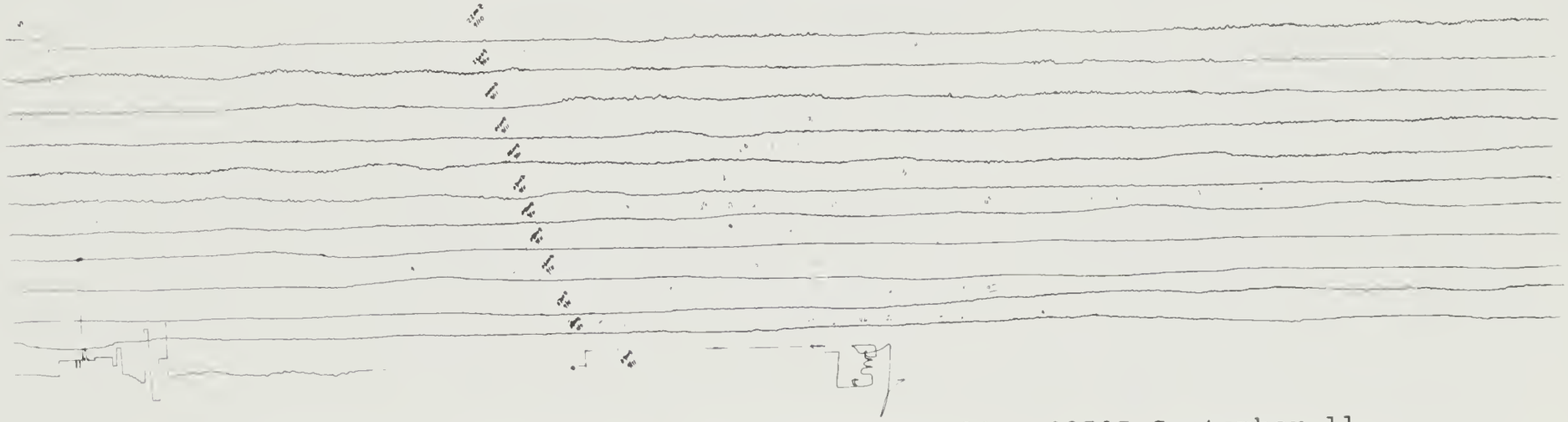

Figure 15. Record 52c. 2145Z September 10 - 0850Z September 11. Thermistor depth - 60 meters.

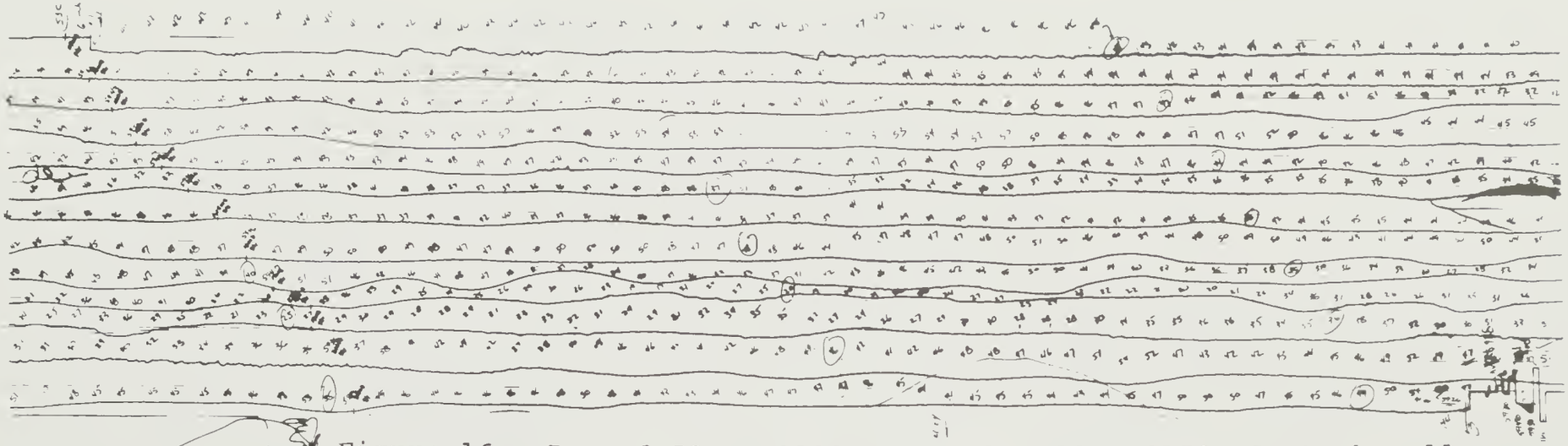

Figure 16. Record 53c. 0900Z September 11 - 2150Z September 11. Thermistor depth - 60 meters.

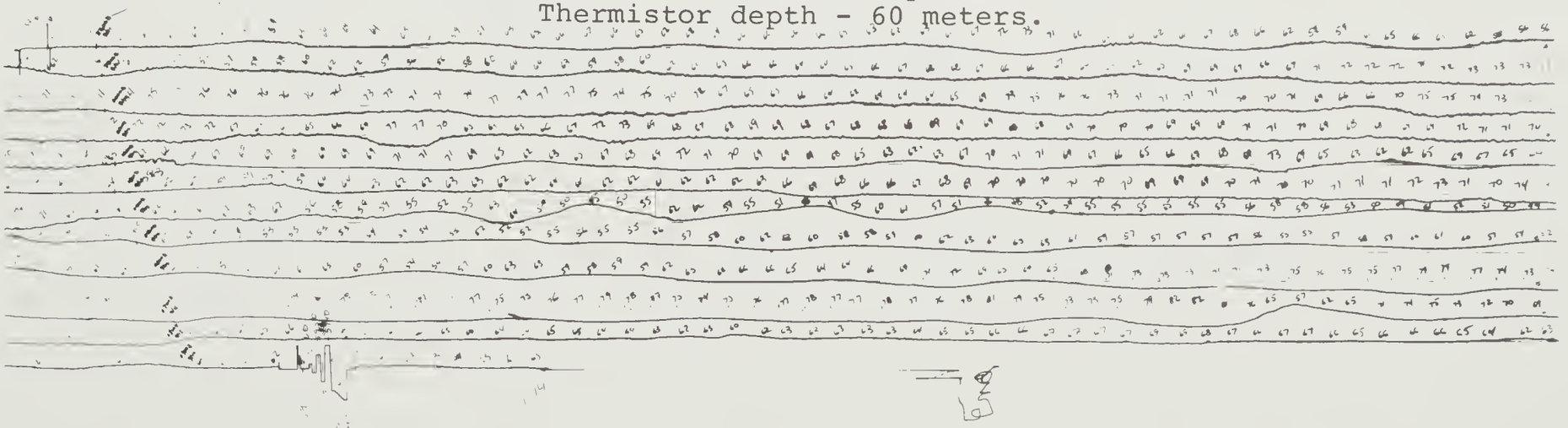

Figure 17. Record 54c. 2200Z September 11 - 0900Z September 12. Thermistor depth - 60 meters.

Figure 18. Record 55c. 0905Z September 12 - 2305Z September 12. Thermistor depth - 60 meters.

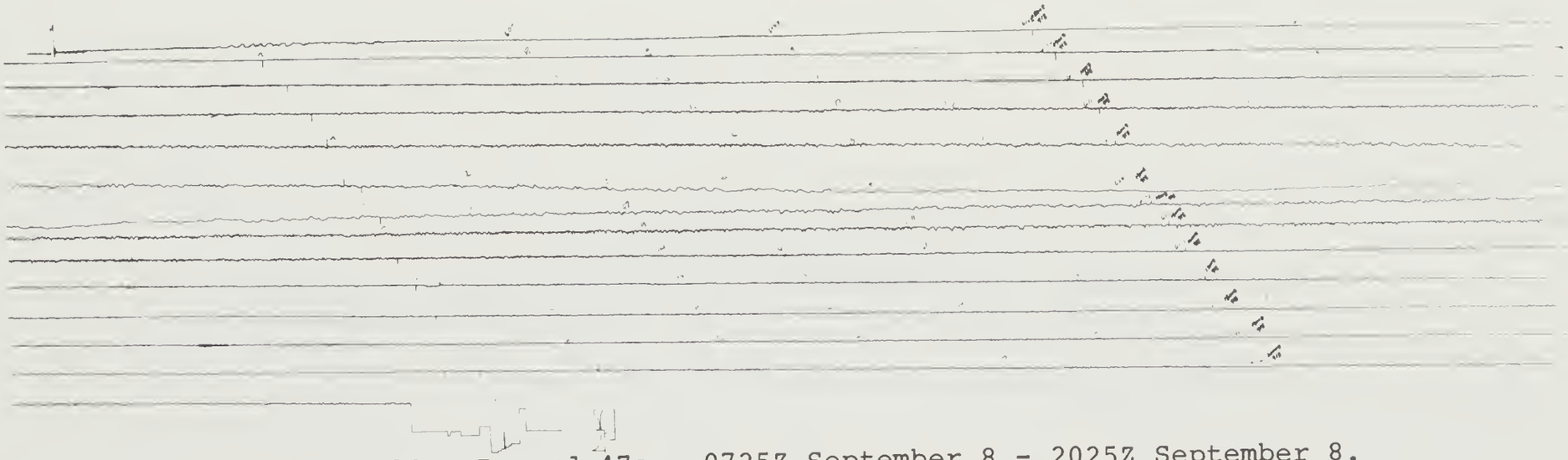

Figure 19. Record 47a. 0725Z September 8 - 2025Z September 8.
Thermistor depth - 125 meters.

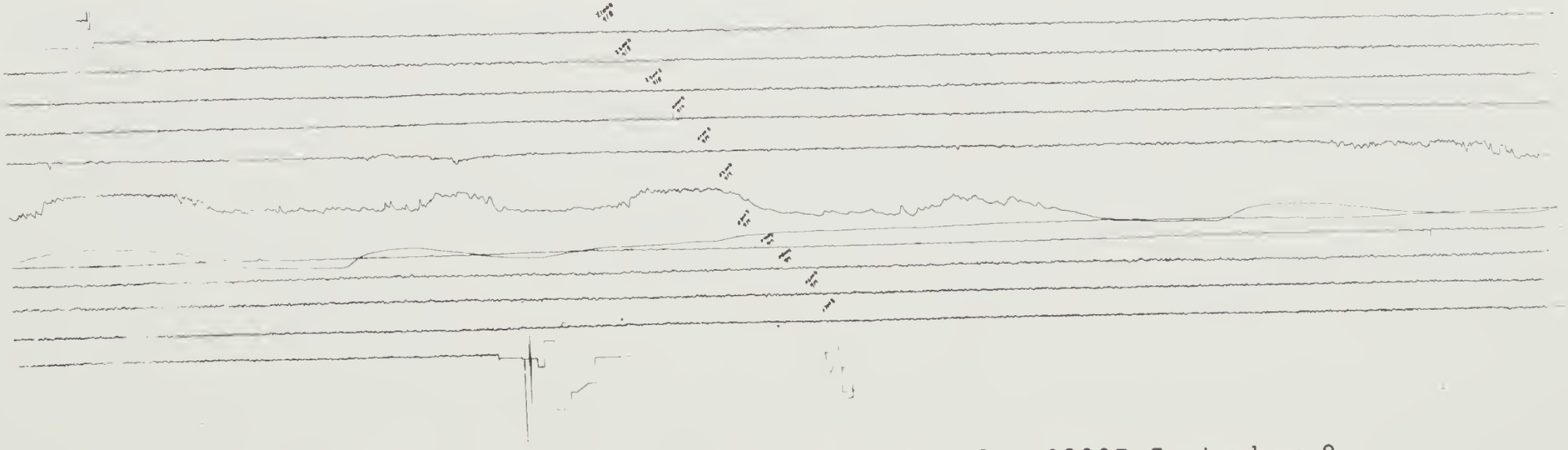

Figure 20. Record 48a. 2040Z September 8 - 0800Z September 9.
Thermistor depth - 125 meters.

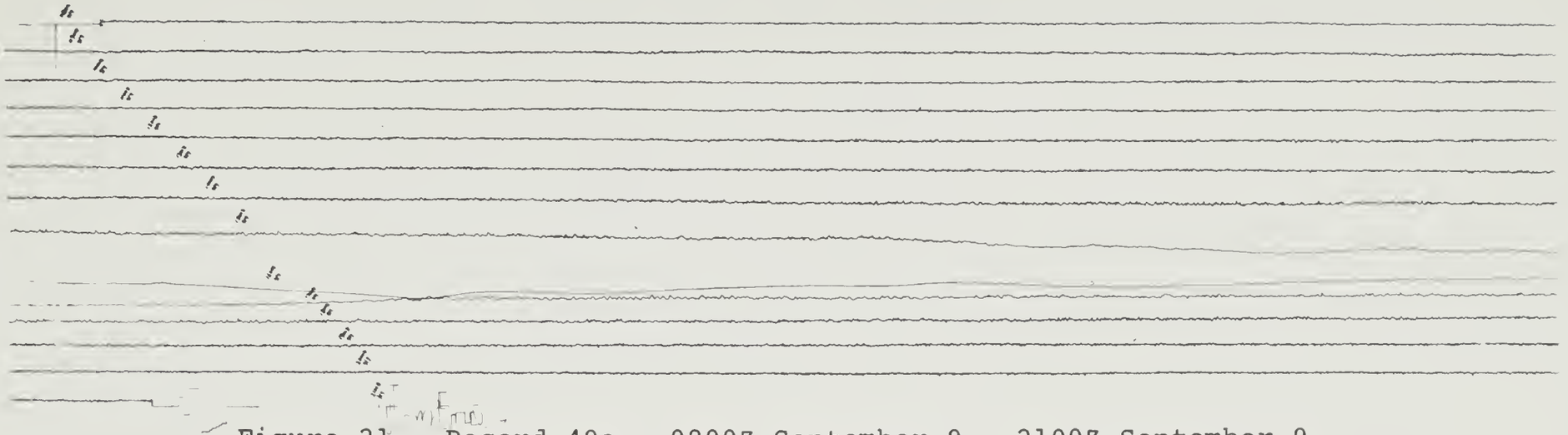

Figure 21. Record 49a. 0800Z September 9 - 2100Z September 9.
Thermistor depth - 125 meters.

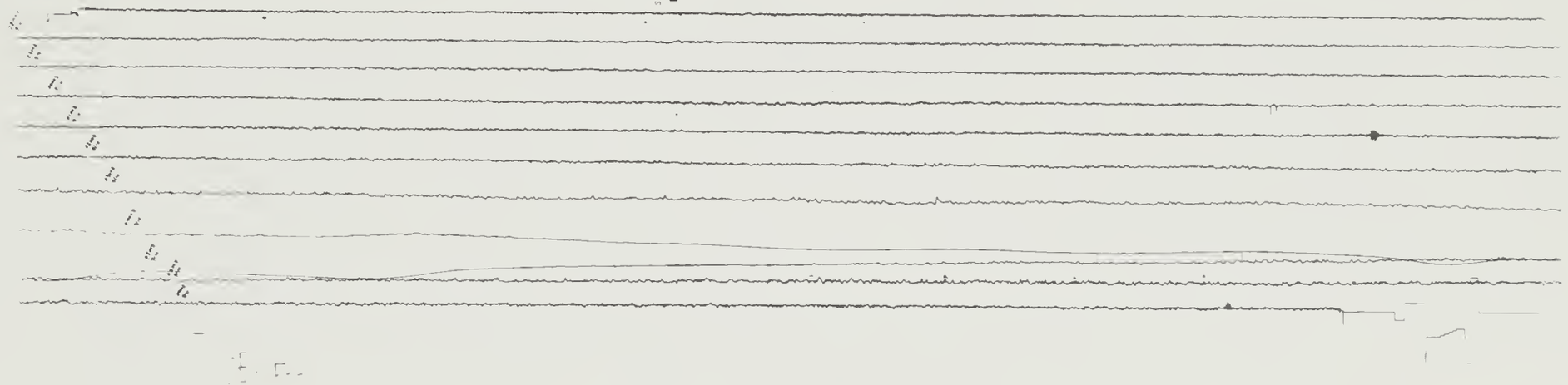

Figure 22. Record 50a. 2100Z September 9 - 0730Z September 10.
Thermistor depth - 125 meters.

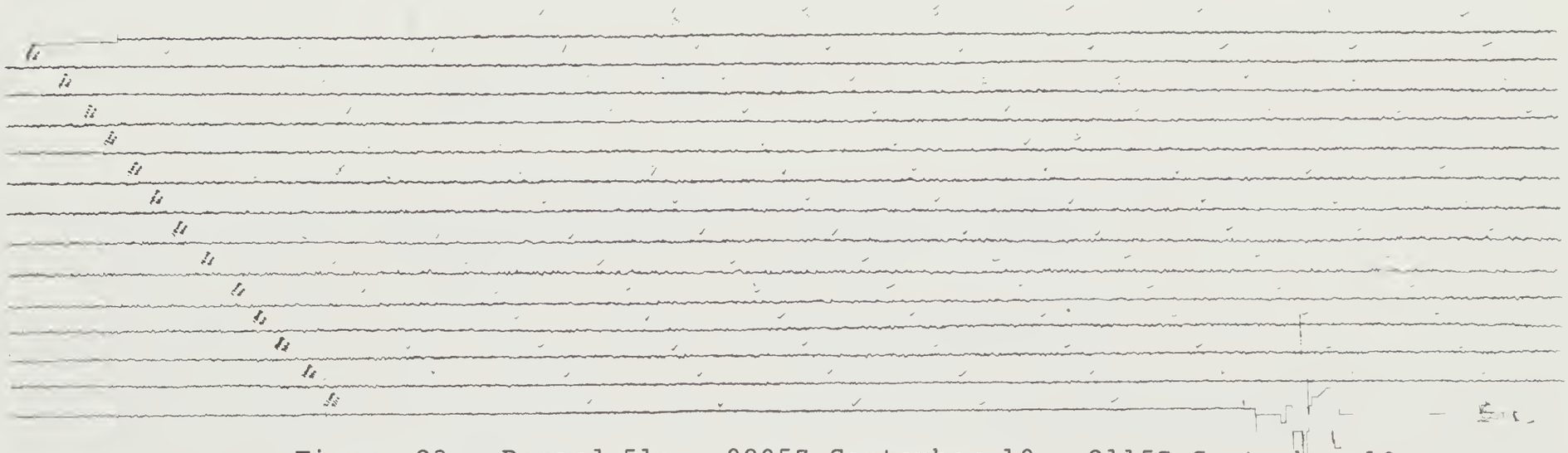

Figure 23. Record 51a. 0805Z September 10 - 2115Z September 10.
Thermistor depth - 125 meters.

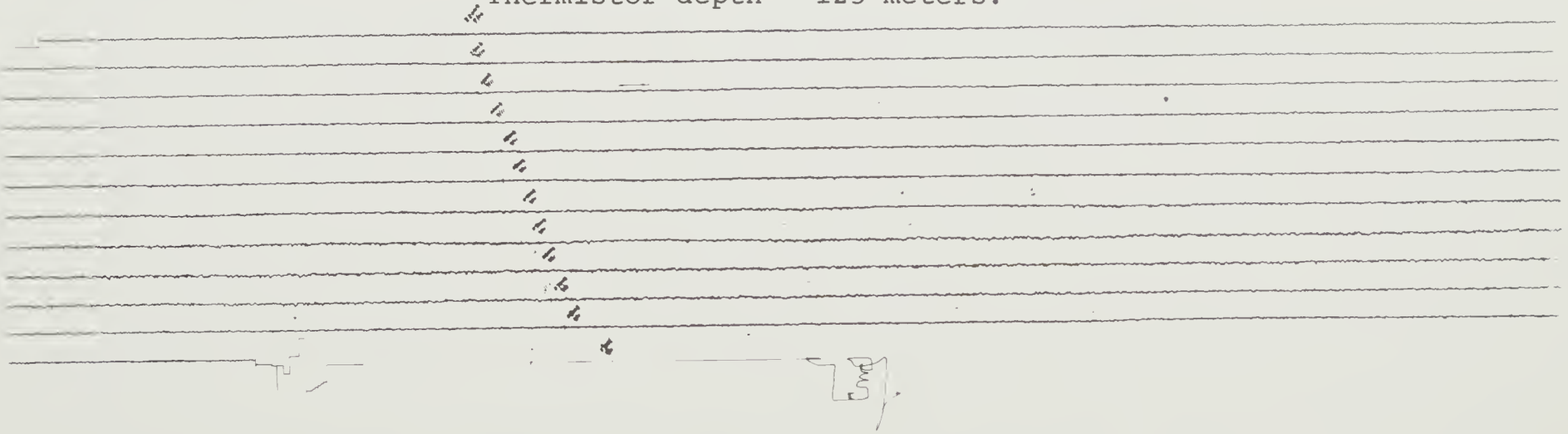

Figure 24. Record 52a. 2145Z September 10 - 0850Z September 11.
Thermistor depth - 125 meters.

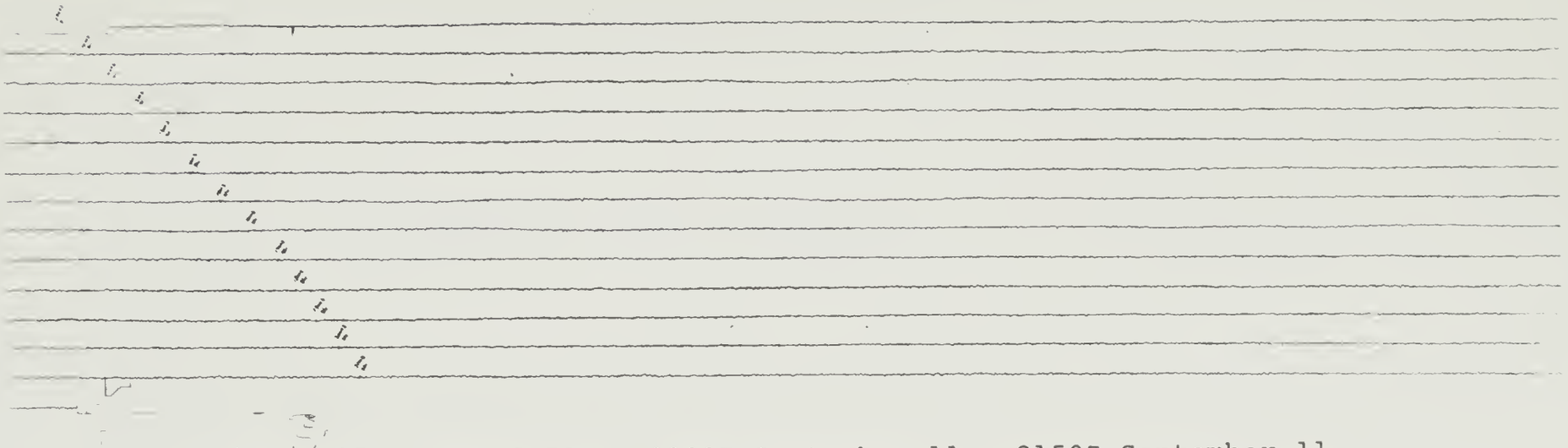

Figure 25. Record 53a. 0900Z September 11 - 2150Z September 11.
Thermistor depth - 125 meters.

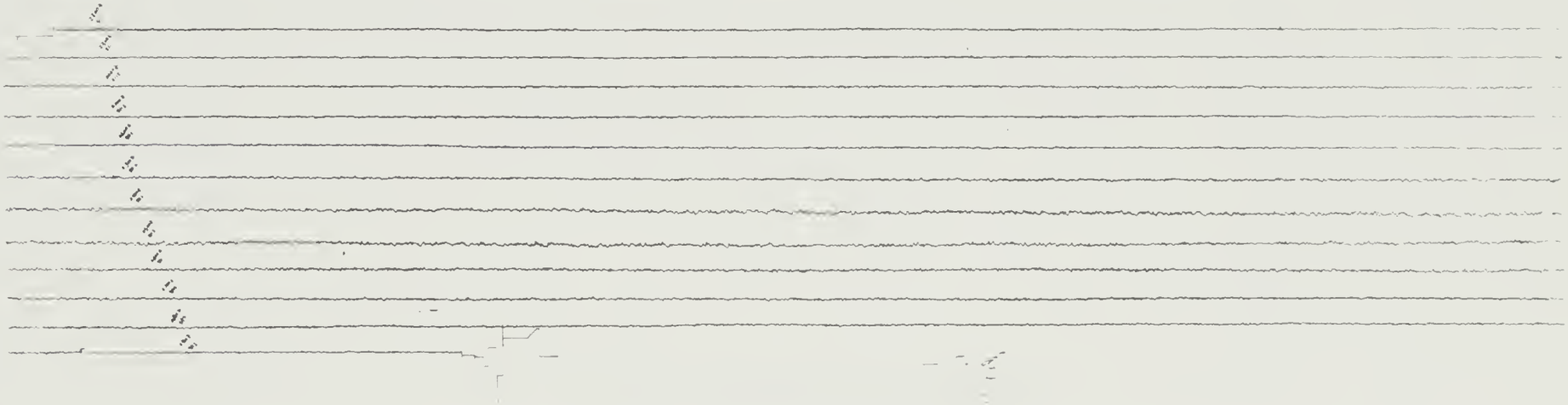

Figure 26. Record 54a. 2200Z September 11 - 0900Z September 12.
Thermistor depth - 125 meters.

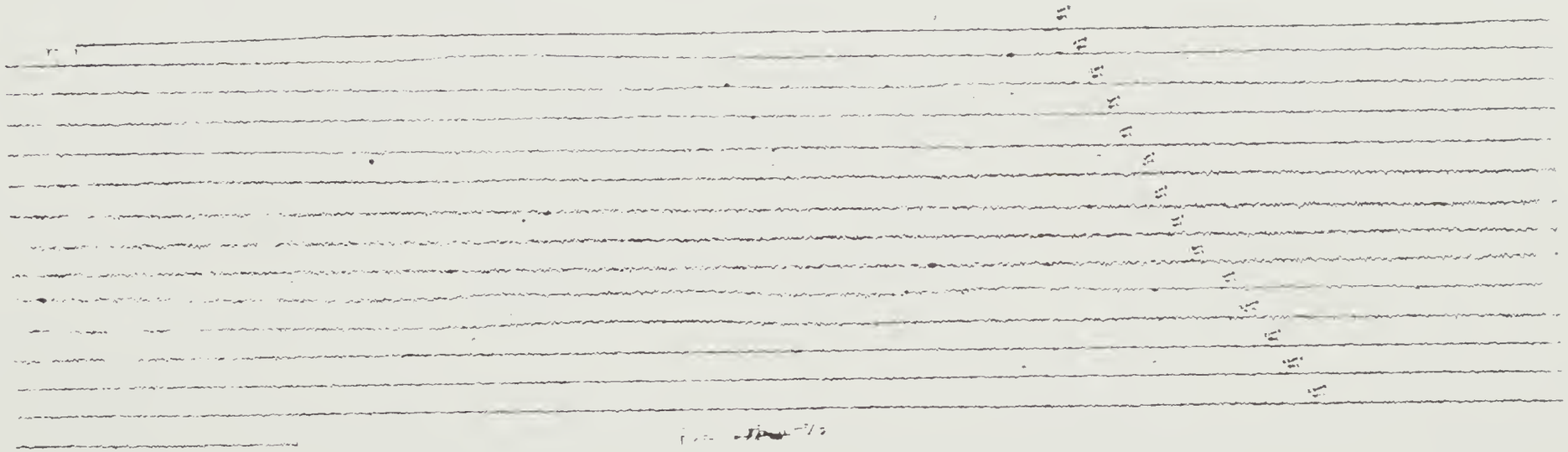

Figure 27. Record 55a. 0905Z September 12 - 2305Z September 12.
Thermistor depth - 125 meters.

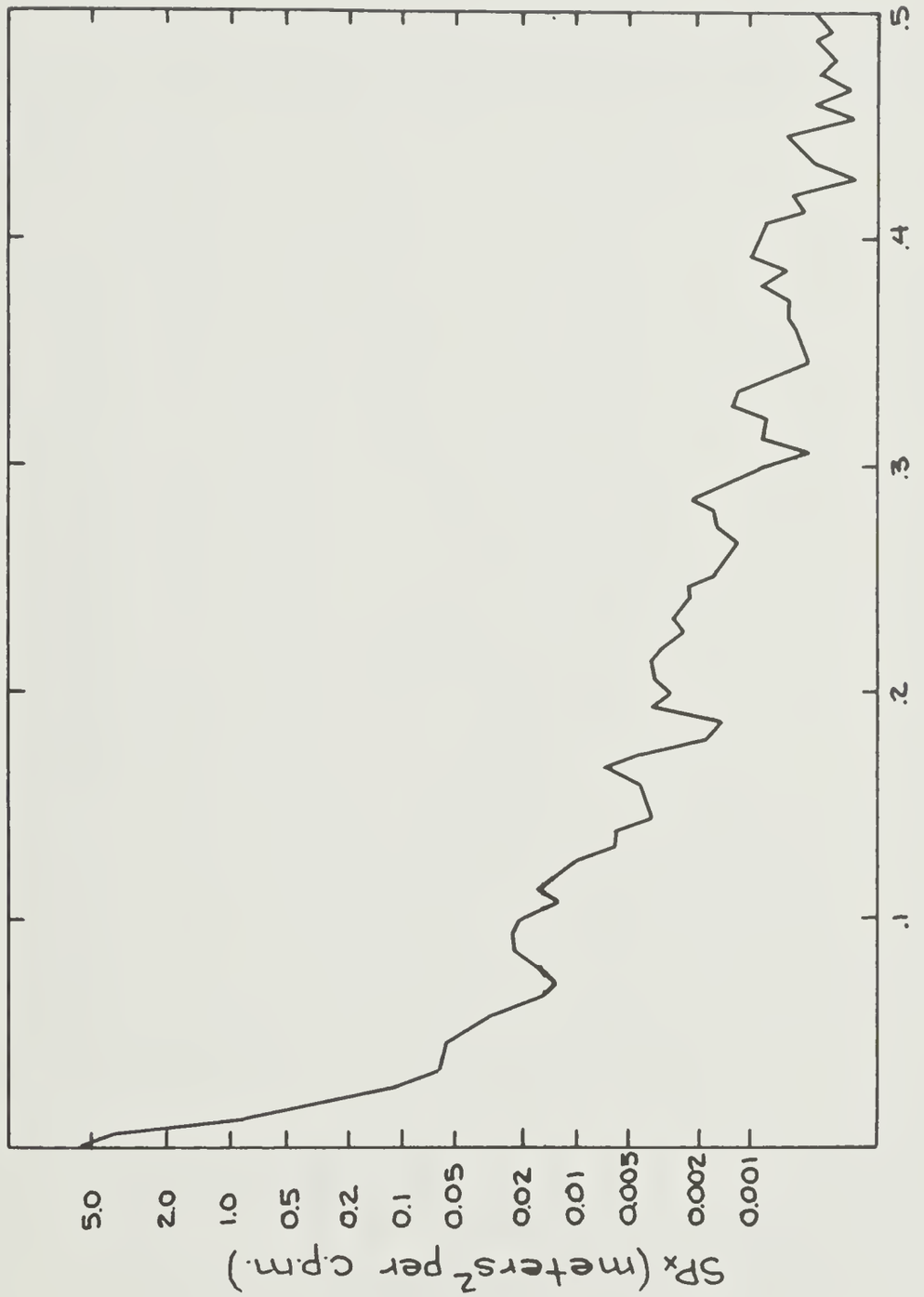

Figure 28. Power spectrum of record 47c.

Figure 29. Power spectrum of record 48c.

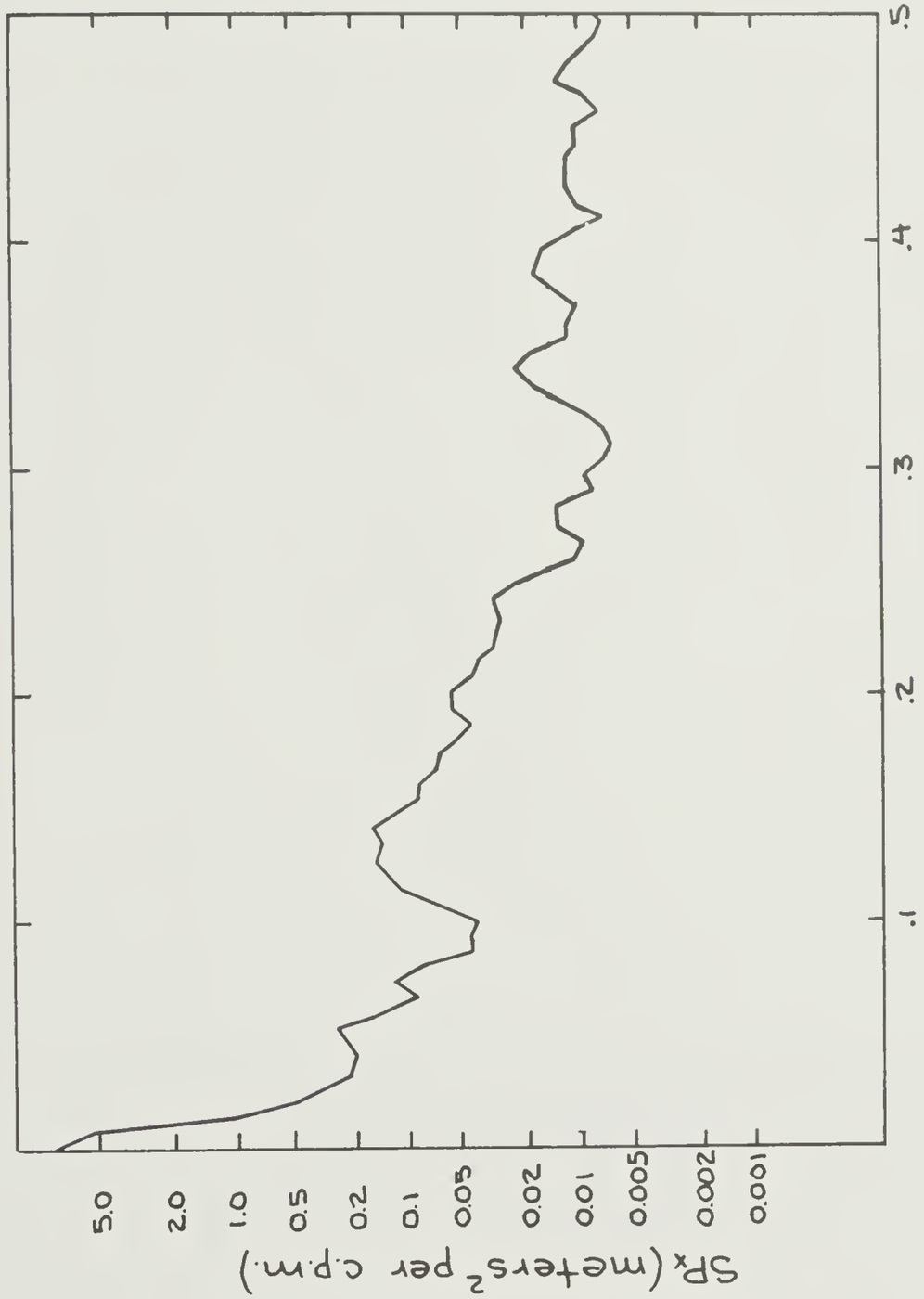

Figure 30. Power spectrum of record 49c.

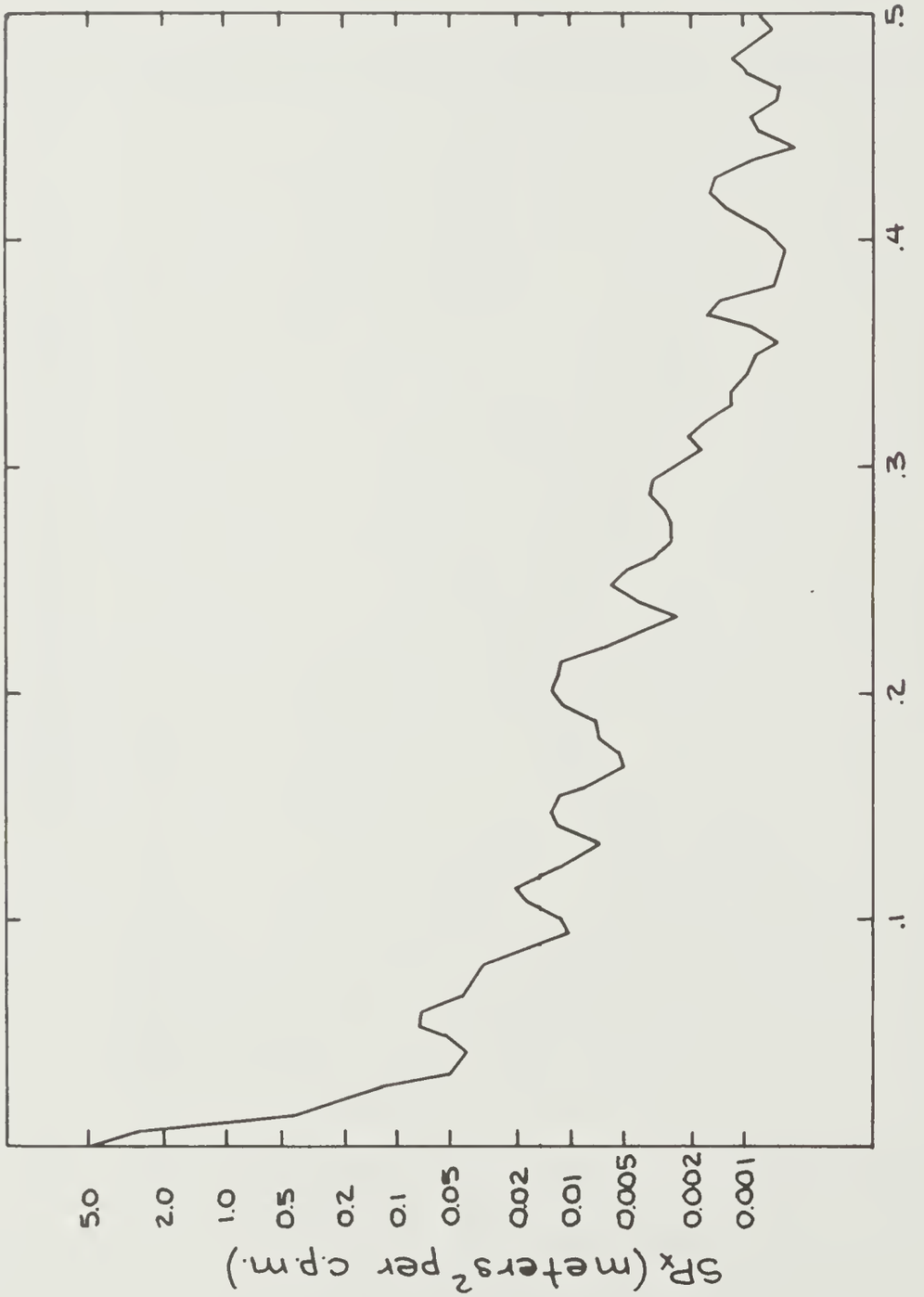

Figure 31. Power spectrum of record 50c.

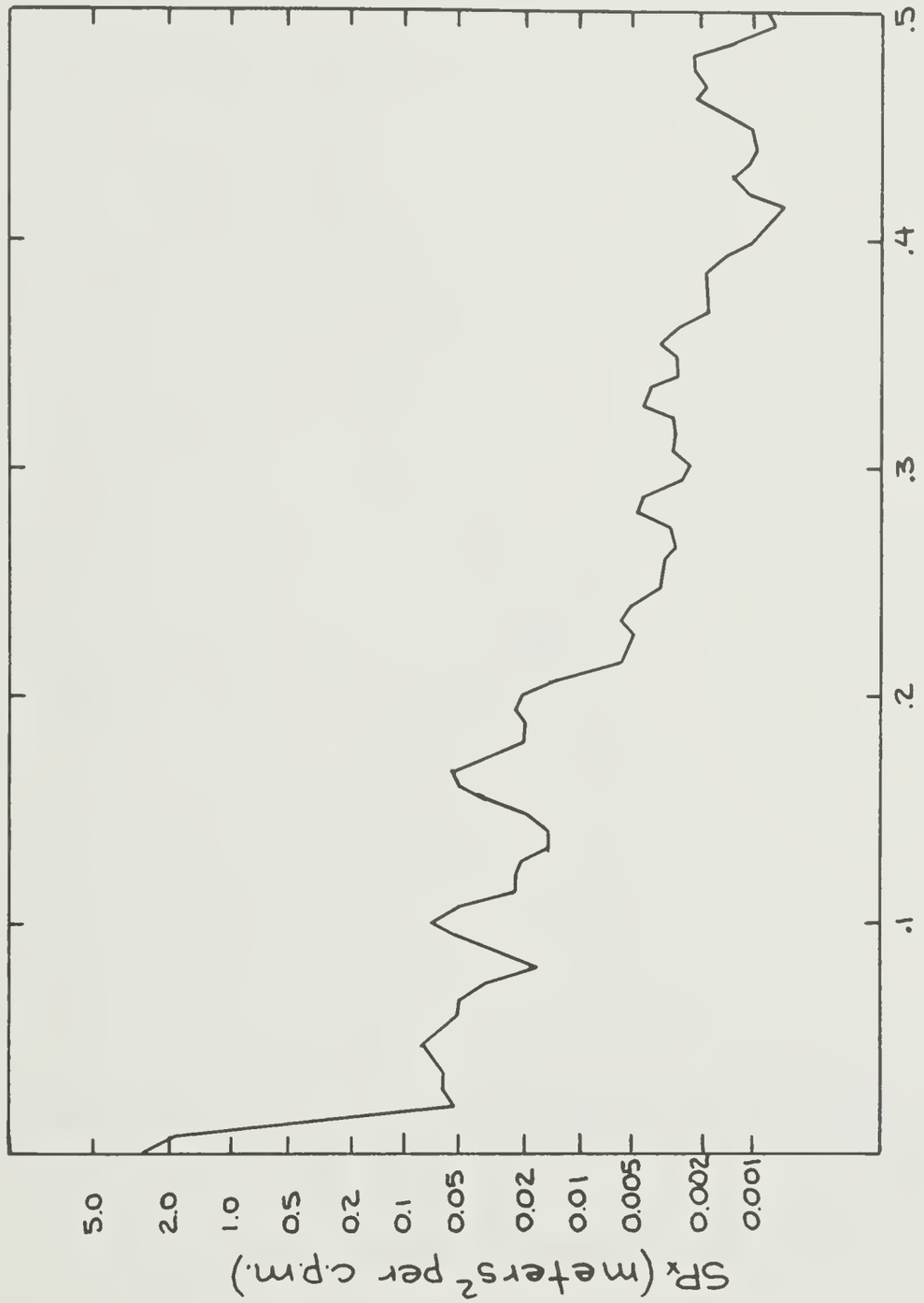

Figure 32. Power spectrum of record 51c.

Figure 33. Power spectrum of record 52c.

Figure 34. Power spectrum of record 53 c.

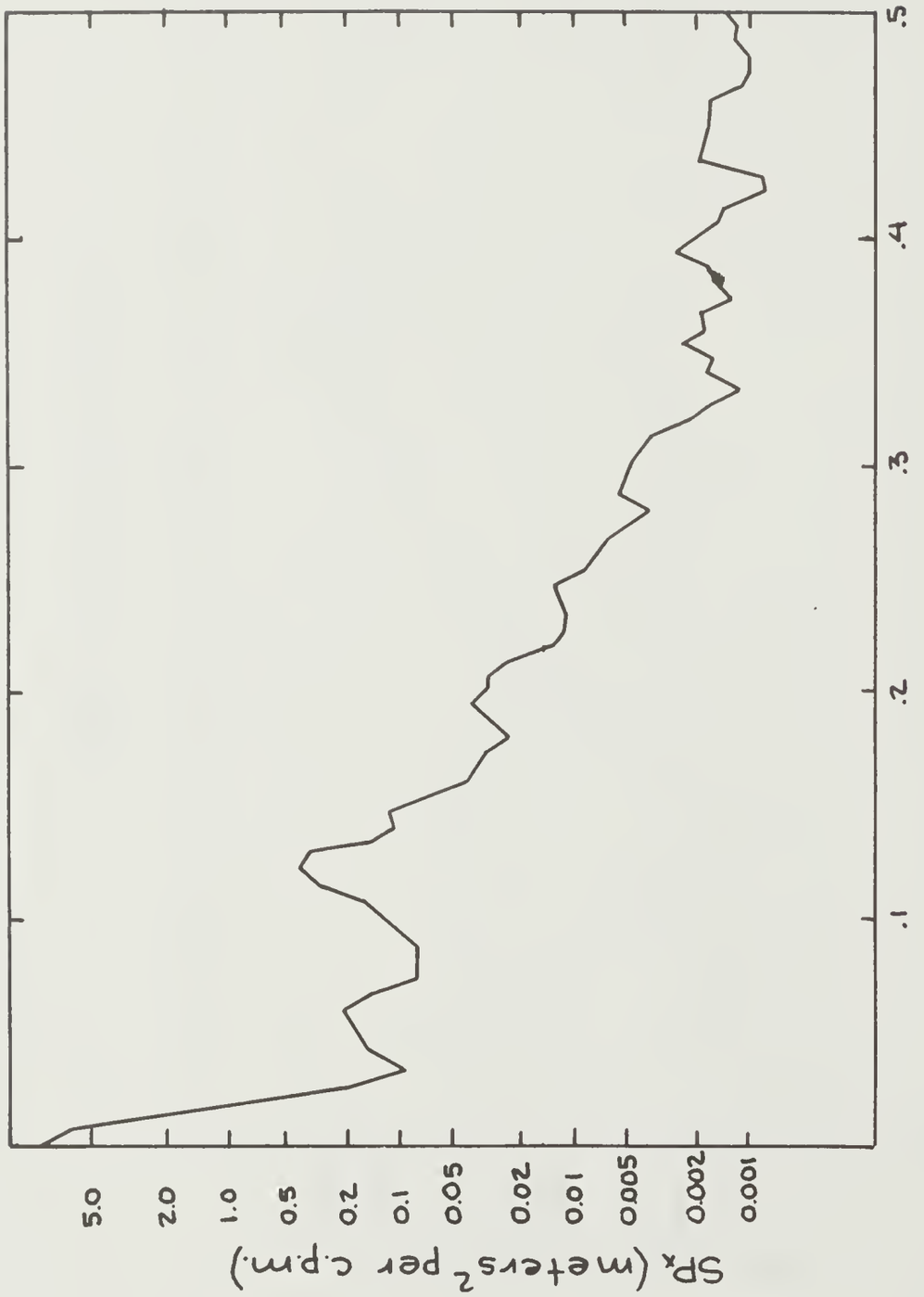

Figure 35. Power spectrum of record 54c.

Figure 36. Power spectrum of record 55c.

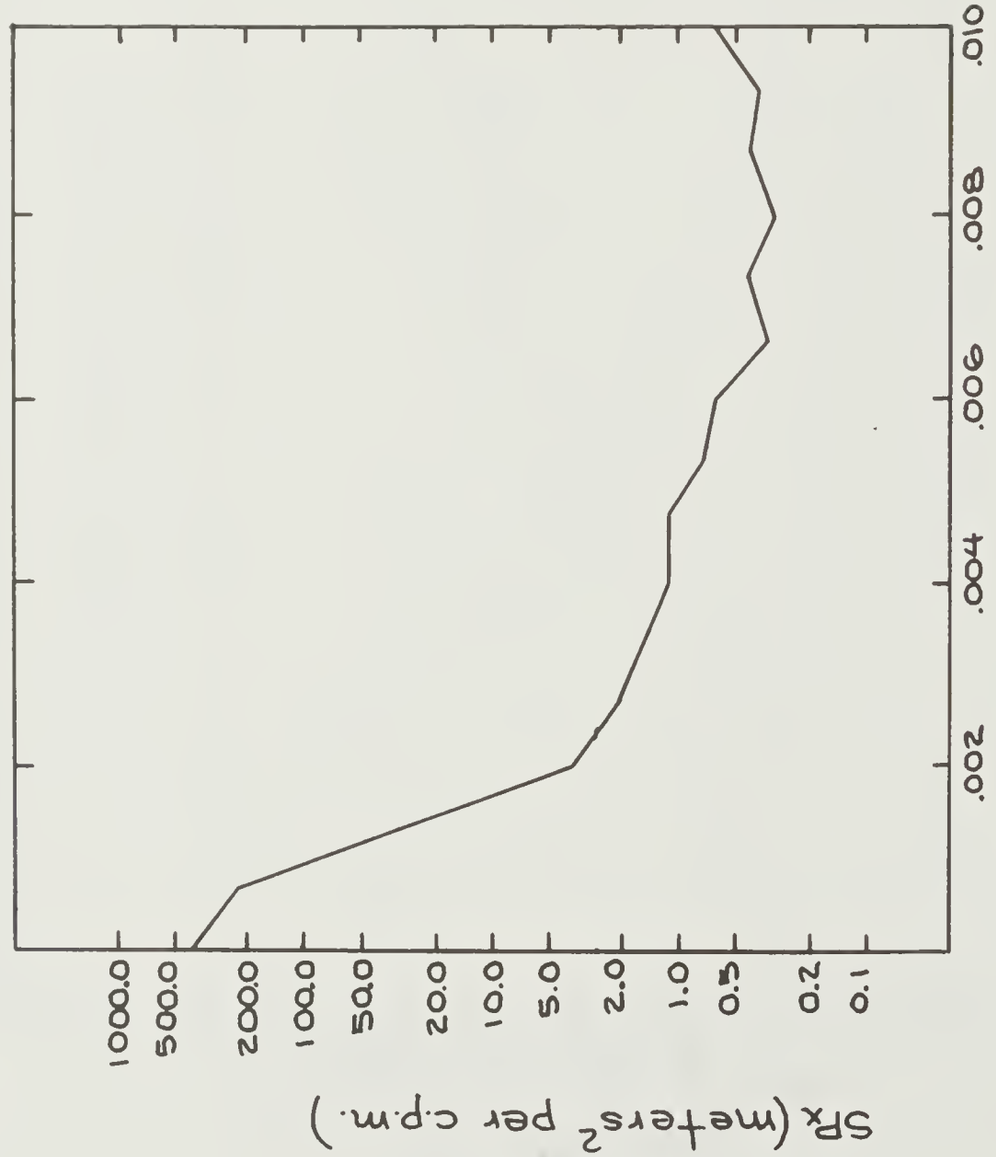

Figure 37. Power spectrum of record 47a.

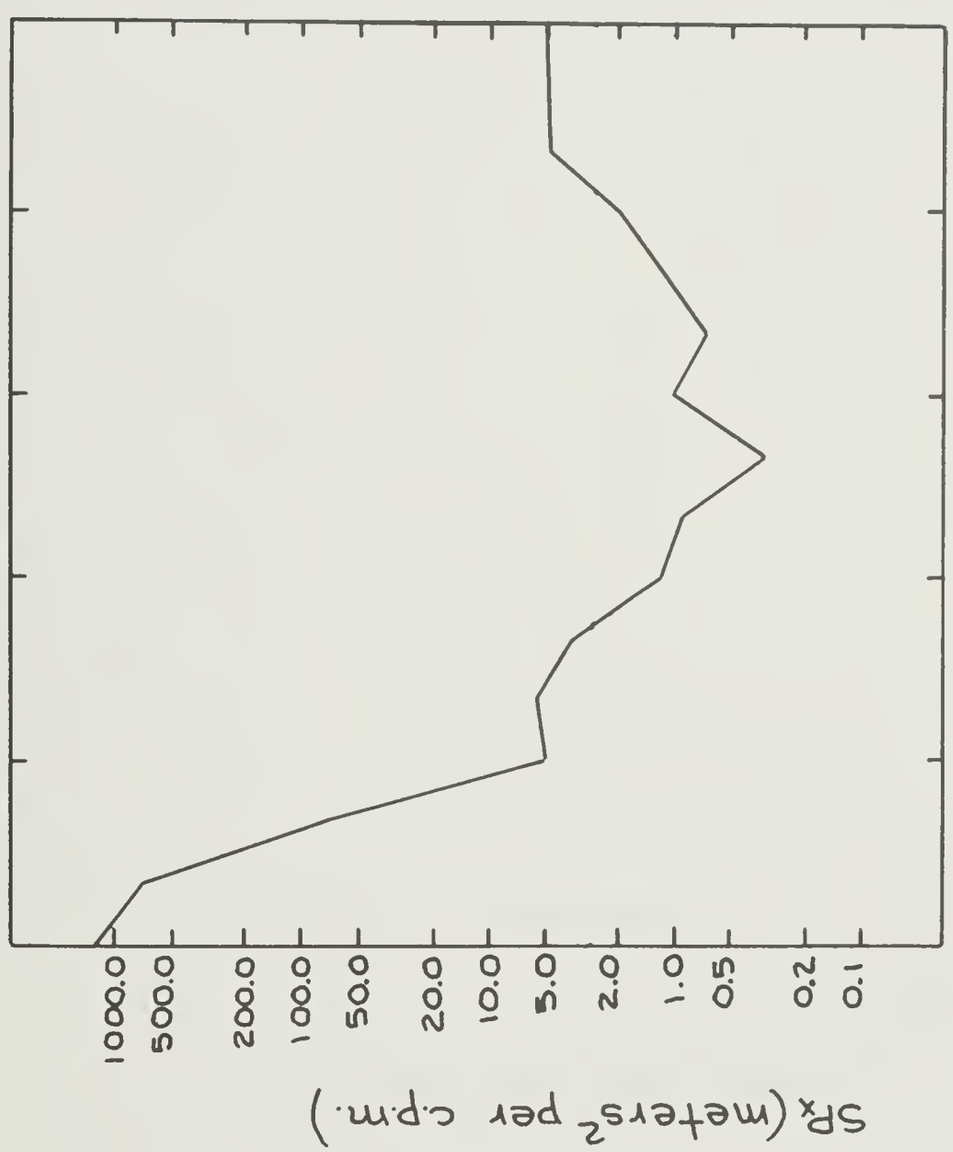

Figure 38. Power spectrum of record 48a.

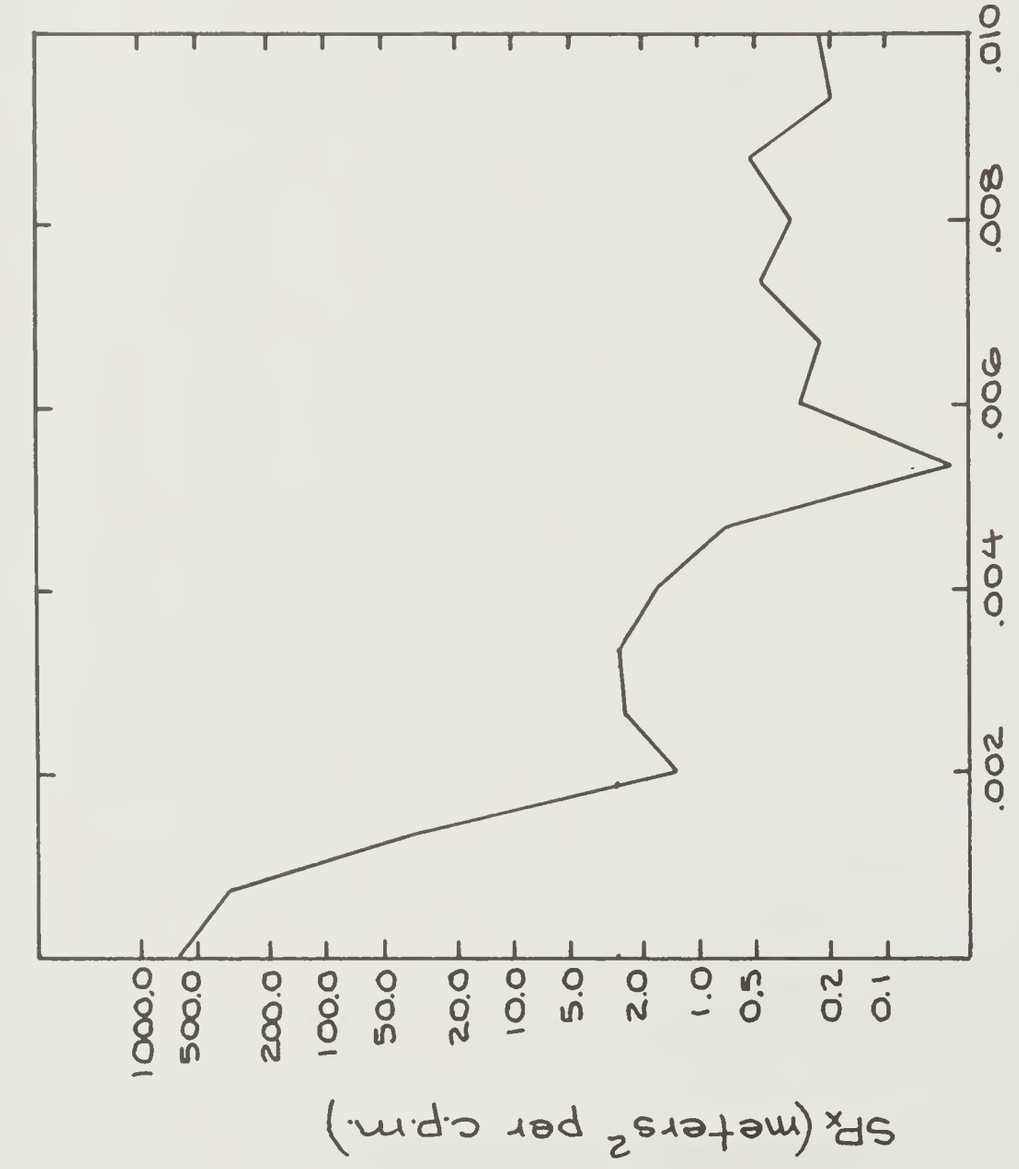

Figure 39. Power spectrum of record 49a.

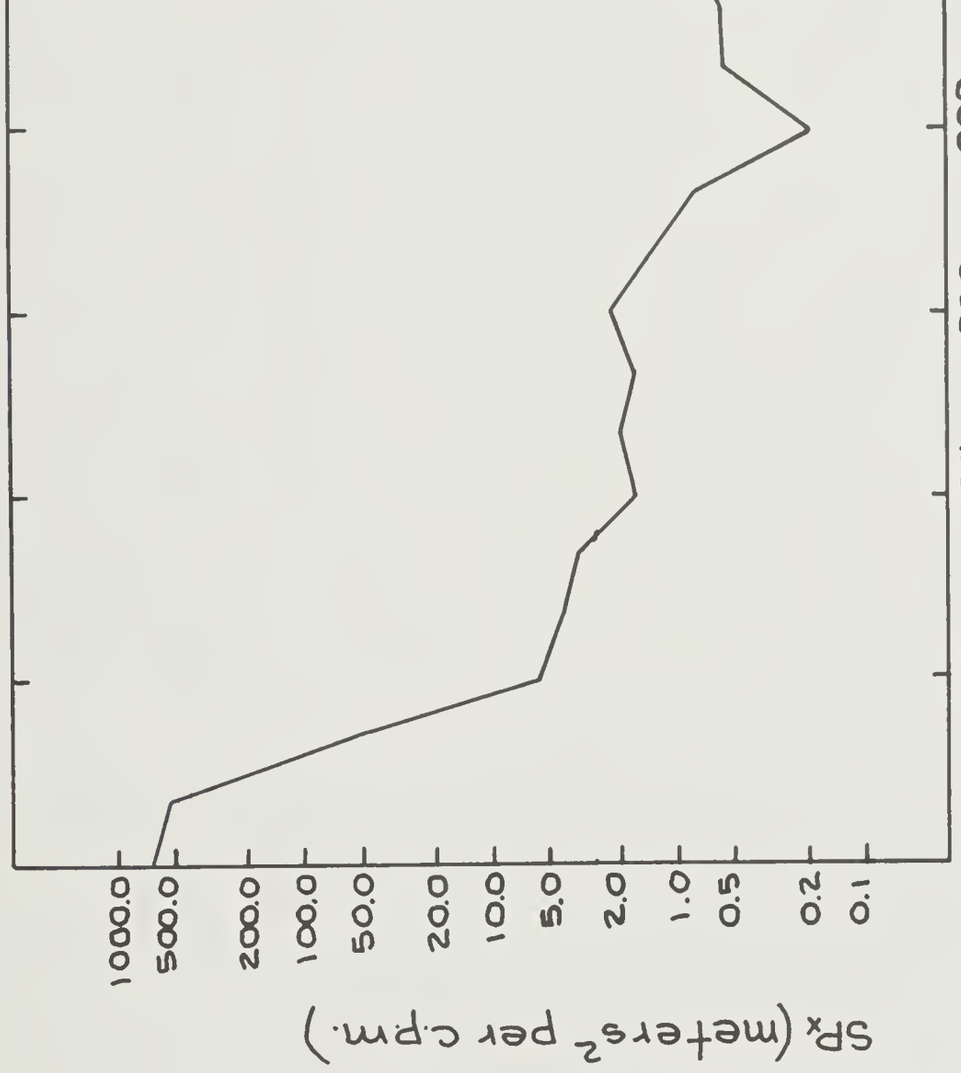

Figure 40. Power spectrum of record 50a.

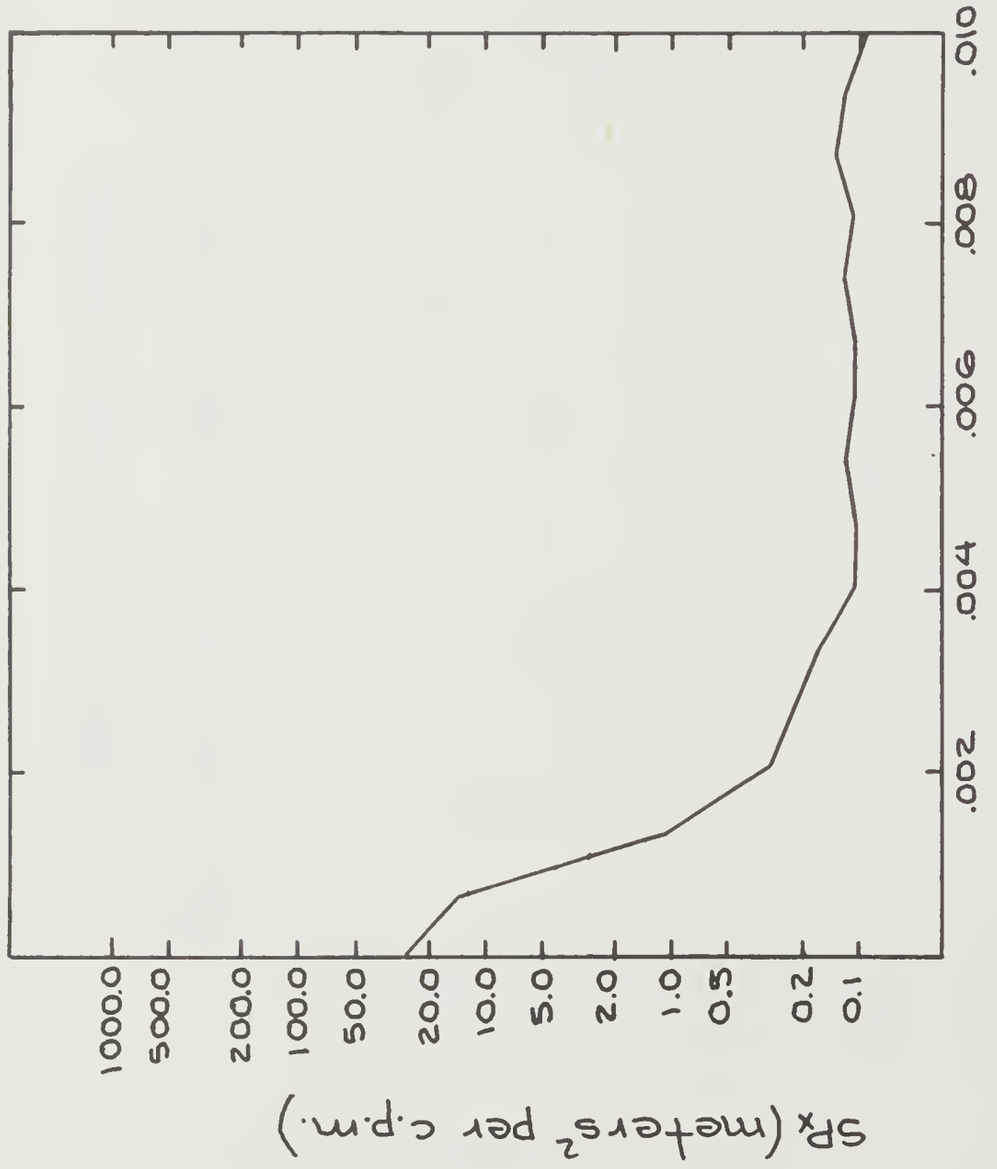

Figure 41. Power spectrum of record 51a.

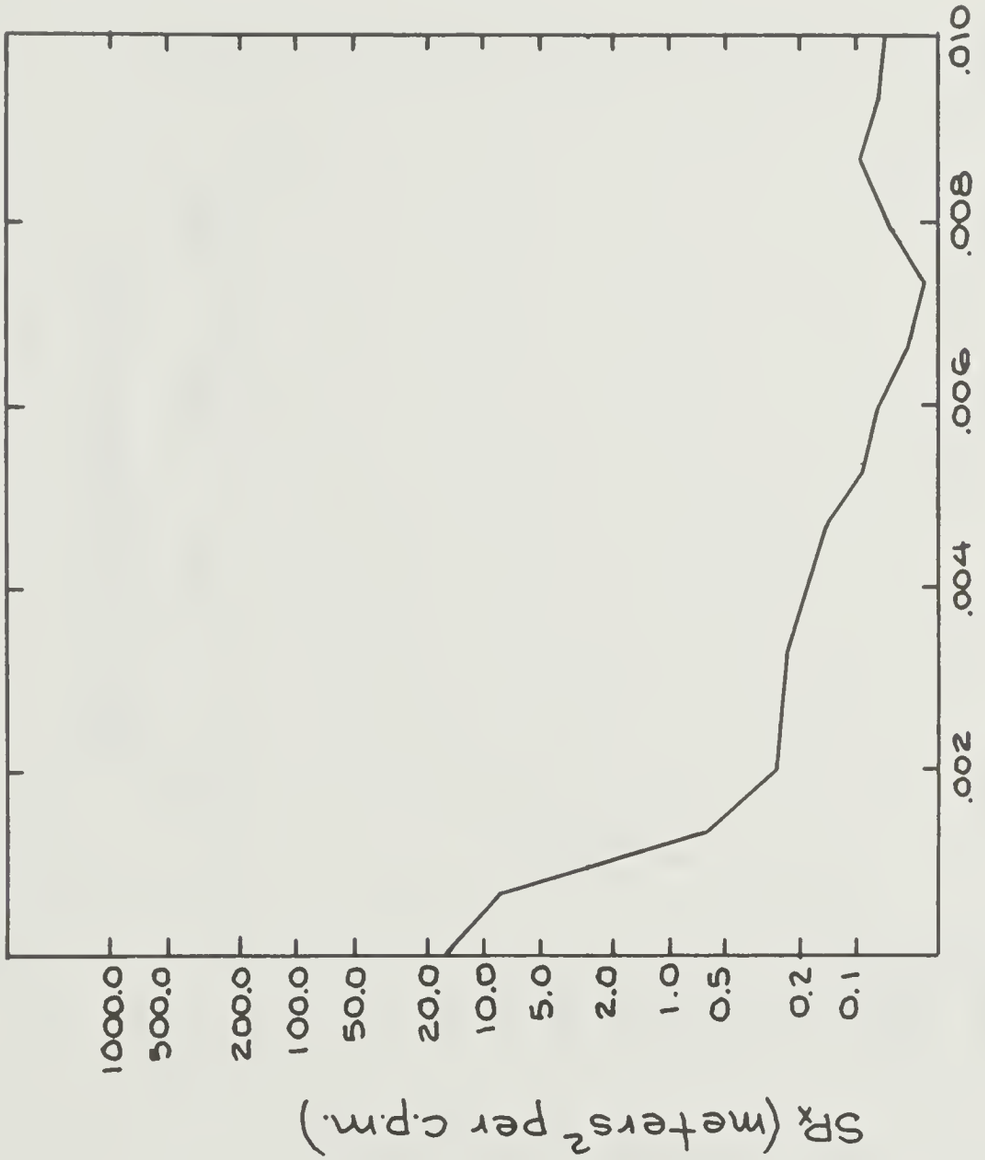

Figure 42. Power spectrum of record 52a.

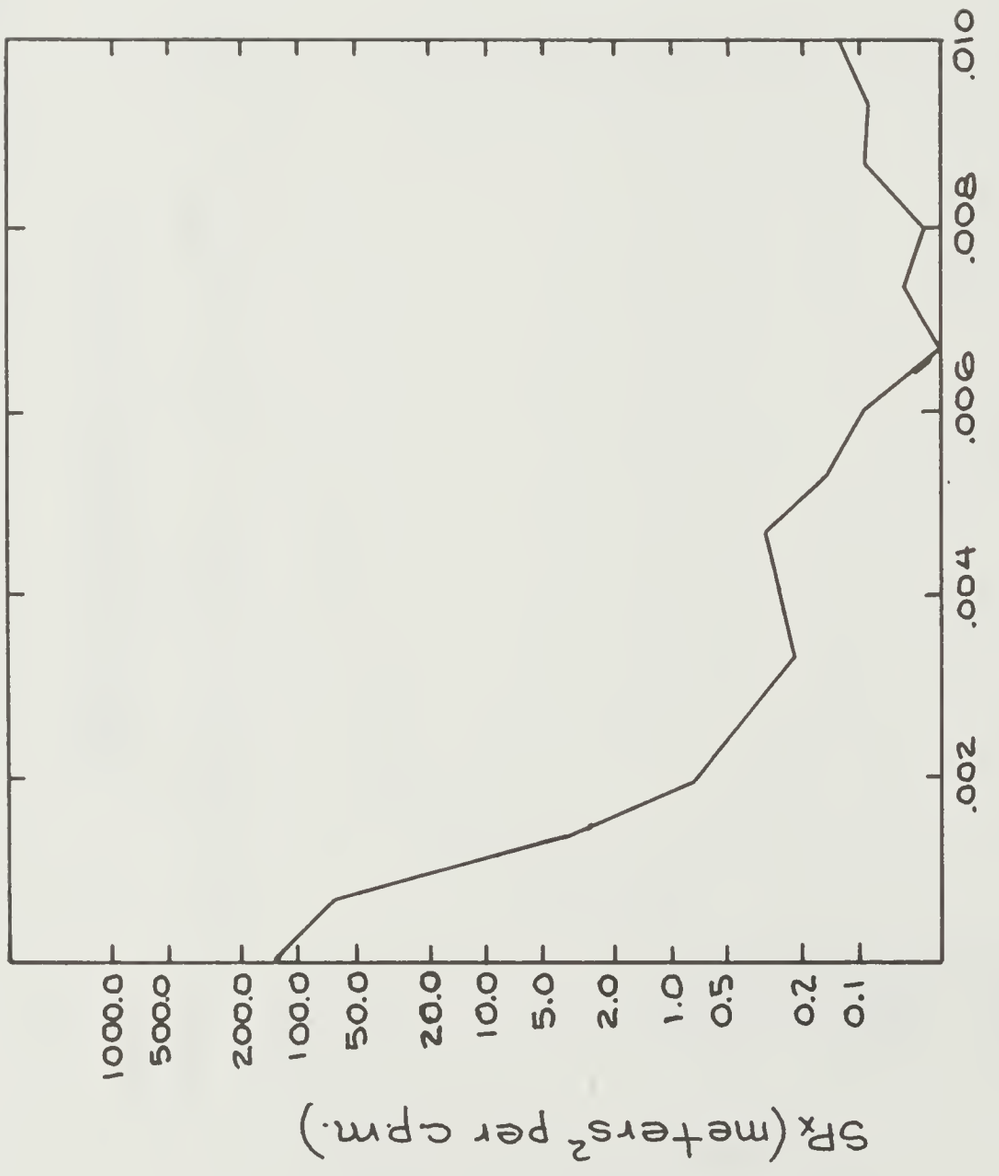

Figure 43. Power spectrum of record 53a.

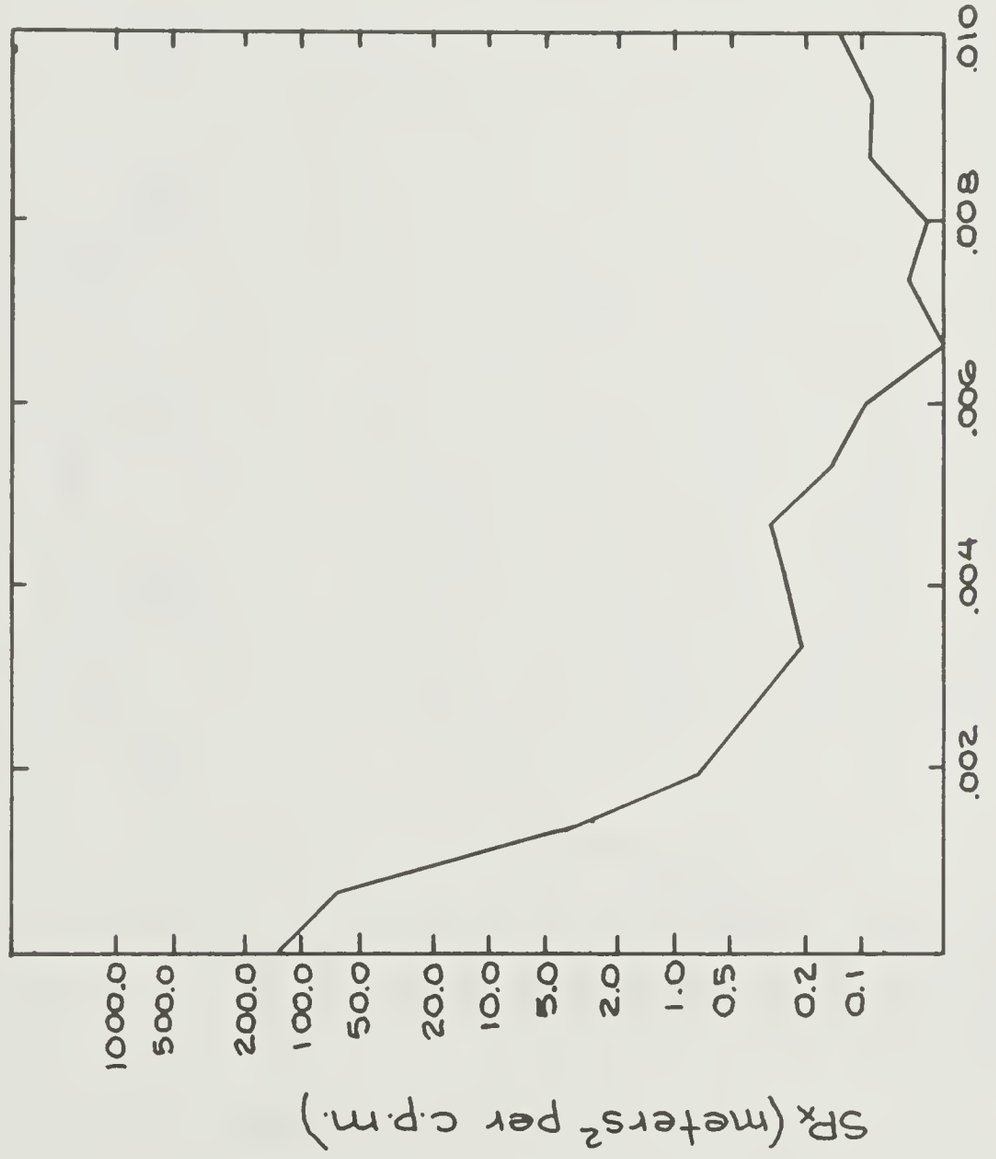

Figure 44. Power spectrum of record 54 a.

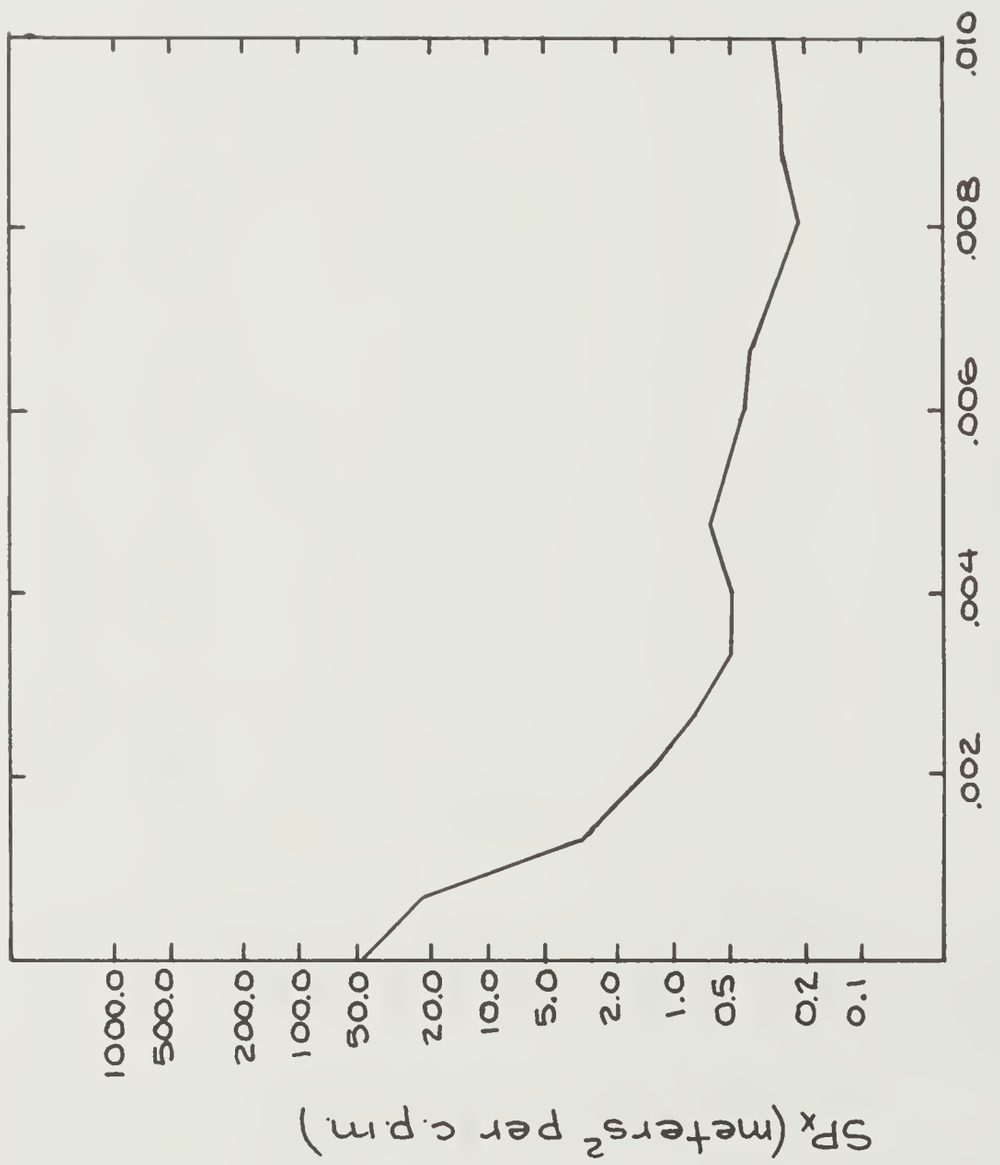

Figure 45. Power spectrum of record 55a.

IV. DISCUSSION OF RESULTS

4.1 Decrease of power with increasing frequency.-- An interesting feature of the spectral estimates (figures 28-45) is the rapid decrease of power with increasing frequency. For frequencies greater than 0.2 c.p.m. at 60 meters (figures 28-36) this decrease is approximately proportional to f^{-3}. For frequencies greater than 0.035 c.p.m. at 125 meters (figures 37-45) the decrease is somewhat less, and is approximately proportional to $f^{-5/2}$. This same phenomenon has been observed by others, notably Haurwitz et al(1959). As these authors have pointed out, the actual decrease may be even sharper for a number of reasons. (1) The smoothing process (equations (3.6.5a,b,c)) used to determine the power spectral estimates results in a diffusion of power from the high points to the low points. (2) Errors in picking off the values from the raw data result in noise which may increase the high frequency values more, in proportion, than the low frequency values.

There are a number of possible explanations for this decrease of power with increasing frequency. Groen(1948) has shown that in a rotating, stratified fluid there is an upper and lower limit on frequencies of internal gravity waves which can propagate. The lower limit is determined by the value of the local Coriolis parameter $f = 2\Omega \sin \Phi$, the upper limit by the maximum value of the Brunt-Väisälä frequency $N = \sqrt{-\frac{g}{\rho_0}\frac{d\rho_0}{dz}}$. The dispersion relation (equation (2.6.6))

obtained previously is consistent with this, and, as can be seen from figure 6, the upper and lower limits on frequency in the Arctic Ocean are 2.0×10^{-2} and 1.4×10^{-4} radians per second, respectively. Therefore, one would expect very little power in frequeniies greater than 2.0×10^{-2} radians per second (.19 c.p.m.).

The work of Hunkins(1962) also provides a basis for explaining, at least qualitatively, the decrease of power with increasing frequency. His work was an analysis of surface wave records in the Arctic, and showed that the amplitude of the surface waves increased with decrease in frequency. If the internal waves are generated by the surface waves the resulting spectrum would be expected to be similar to the surface wave spectrum. This argument assumes, of course, that the coupling is the same for all wave-lengths, and also ignores the effects of resonances. Actually, it would be expected that the efficiency of the coupling would be greater for the longer wave-lengths (lower frequencies).

4.2 The spectral peak at .08-.12 c.p.m.-- The power spectral extimates of the 60-meter records all show a distinct peak in the region from .08 to .12 c.p.m. In the first three records (figures 28, 29 and 30) and, to a lesser extent, in the others this peak appears to shift with time toward the higher frequencies. This may be due to a Doppler effect caused by the relative motion between island and ocean, which, for these frequencies, would be of the order of 10% for an island motion of 10 cm./sec. During the experiment the relative

motion was of the order of 1-5 cm./sec., as estimated from pressure transducer wire-angle. The shifting of the spectral peaks with time may also be due to the dispersion of the waves travelling from a distant source.

Hunkins(1962) states that the surface waves in this portion of the spectrum are generated by local winds and, assuming that the internal waves are coupled to the surface waves, the internal waves probably have a similar origin.

4.3 The very high frequency oscillations.-- As mentioned in paragraph 3.5 the raw data was smoothed by eye to eliminate the very high frequency oscillations. These oscillations, from a visual examination only, are found at frequencies greater than approximately 2 c.p.m. As can be observed in a number of the raw data records (figures 10 and 11, for example) the amplitudes of these oscillations are of the same order as the lower frequency motions for which power spectra were calculated. At other times these very high frequencies are barely observable. The distinct gap in the spectrum and the random manner in which these very high frequency oscillations occur would suggest that they are of an essentially different nature than the lower frequency oscillations.

Electrical noise in the EMF driving the output pen may have been responsible for some of these motions. However, when the thermistor was replaced in the bridge by the decade box the very high frequency oscillations were not observed. It is possible that the motion of the thermistor cables through

the Earth's magnetic field could have generated sufficient EMF to cause these very high frequency oscillations. It is interesting to note that data taken by A. Hansen of the University of Washington's Department of Atmospheric Sciences (personal communication) on a mechanically-driven "tide gauge" show similar motions in the very high frequency range mentioned above. This "tide gauge" measured the relative displacement of the surface level with respect to the island. This provided a record of surface motion analogous to the measurements in this work, which were internal motions relative to the ice island.

These very high frequencies may also be a result of turbulence, but until further experiments are conducted it will be difficult to be certain.

4.4 Recommendations.-- The results of this work indicate the presence of internal waves in the deep Arctic Ocean. To determine the amplitudes of the individual modes, the kinetic and potential energy as a function of frequency, effects of friction, phase velocity and the source of the internal waves will require instrumentation in greater quantity than was used in this experiment. A triangular grid of three vertical arrays with five to six thermistors in each vertical array would perhaps be sufficient.

At present, a major problem is determining the position and velocity of the island with sufficient accuracy. Before any extended work is begun it will be necessary to solve this problem. A number of methods are available, one of which is

being used at present. The group under Dr. L. K. Coachman of the University of Washington's Department of Oceanography is testing a drift meter which uses a 12 kilocycle "pinger" resting on the ocean bottom. The difference in travel time of the "ping" to three hydrophones located on the pack ice determines the island motion. This device has been used with some success on ARLIS II, but, as yet, has not given satisfactory results on T-3. Another method of position control under consideration is satellite navigation, and a receiver may be available for use in the Arctic within a year or two.

Digital temperature-recording equipment for the thermistor arrays will also be necessary. The necessity of reducing the data manually would be eliminated and longer records could be analyzed rapidly and accurately. This type of equipment is available commercially at present, and future work in internal waves in the Arctic will benefit by its use.

BIBLIOGRAPHY

Blackman, R. B., and J. W. Tukey
1958. The measurement of power spectra. Dover Publications, New York.

Coachman, L. K.
1963. Water masses of the Arctic. In Proceedings of the Arctic Basin symposium, October 1962, pp. 142-168. Tidewater Publishing Corp., Centerville, Maryland.

Ekman, V. W.
1906. On dead water. The North Polar Expedition, 1893-1896, Scientific Results (F. Nansen, ed.), 5(15), Longmans Green.

Fjeldstad, J. E.
1933. Interne wellen. Geofys. Publ., 10(6).

1964. Internal waves of tidal origin. Geofys. Publ., 25(5).

Groen, P.
1948. Contributions to the theory of internal waves. Koninklijk Nederlands Meteorologisch Institut de Bilt. Mededelingen en Verhandelingen, Ser. B, 2(11).

Haurwitz, B.
1948. The effect of ocean currents on internal waves. J. Mar. Res., 7(3):217-228.

1950. Internal waves of tidal character. Trans. Amer. Geophys. Un., 31(1):47-52.

Haurwitz, B., W. H. Munk, and H. M. Stommel
1959 On the thermal unrest in the ocean. In the Rossby Memorial Volume (B. Bolin, ed.), pp. 74-94. Rockefeller Institute Press, New York.

Helland-Hansen, B., and F. Nansen
1909. The Norwegian Sea. In Norway Fiskeridirektoratet, Report on Norwegian Fishery and Marine Investigations, Vol. 2, pp. 87-132.

BIBLIOGRAPHY

Hunkins, K.
1962. Waves on the Arctic Ocean. J. Geophys. Res., 67(6):2477-2489.

Kline, M.
1948. Some Bessel equations and their application to guide and cavity theory. J. Math. and Phys., 27(1):33-39.

Lee, O. S.
1961. Observations on internal waves in shallow water. Limnology and Oceanography, 6(3):312-321.

Rattray, M., Jr.
1957. Propagation and dissipation of long internal waves. Trans. Amer. Geophys. Un., 38(4):495-500.

1960. On the coastal generation of internal tides. Tellus, 12(1):54-62.

Reid, J. L., Jr.
1962. Observations of inertial rotation and internal waves. Deep-Sea Research, 9(2);283-289.

Stokes, G. G.
1849. On the theory of oscillatory waves. Camb. Phil. Soc., 8(4):441-455.

Worthington, L. V.
1953. Oceanographic results of project Skijump I and Skijump II in the Polar Sea, 1951-1952. Trans. Amer. Gophys. Un., 34(9):543-551.

ACKNOWLEDGMENT

Logistic support was furnished by Arctic Research Laboratory, Barrow, Alaska. This work was supported by Contract Nonr 266 (82) under Project Vela of the Advanced Research Projects Agency.

APPENDIX I

Order of magnitude analysis for the vertical equation.-- Consider the terms:

$$\text{I.} \quad \left[\frac{1}{\rho_0}\frac{d\rho_0}{dz}\right]^2$$

$$\text{II.} \quad \left[\frac{1}{\rho_0}\frac{d^2\rho_0}{dz^2}\right]$$

$$\text{III.} \quad \left[\frac{g}{\rho_0}\frac{d\rho_0}{dz} + \omega^2\right]\left[\frac{k^2}{\omega^2 - f^2}\right]$$

Then if $1/\alpha$ is the characteristic depth of the in situ density profile and A is the ratio of the maximum density change to the maximum density, the conditions under which terms I. and II. can be neglected with respect to term III. are:

$$1. \left[\frac{g}{\alpha A}\right]\left[\frac{k^2}{\omega^2 - f^2}\right] >> 1$$

$$2. \left[\frac{g}{\alpha}\right]\left[\frac{k^2}{\omega^2 - f^2}\right] >> 1$$

or:

$$1. \left[\frac{1}{\alpha^2 A^2}\right]\left[\frac{\omega^2 k^2}{\omega^2 - f^2}\right] >> 1$$

$$2. \left[\frac{1}{\alpha^2 A}\right]\left[\frac{\omega^2 k^2}{\omega^2 - f^2}\right] >> 1$$

For the Arctic Ocean, typical values of the above quantities indicate that the error in neglecting terms I. and II. is of the order of one part in 10^3.

Unclassified

Security Classification

DOCUMENT CONTROL DATA - R&D

(Security classification of title, body of abstract and indexing annotation must be entered when the overall report is classified)

1 ORIGINATING ACTIVITY *(Corporate author)*
Lamont Geological Observatory
Columbia University
Palisades, New York

2a REPORT SECURITY CLASSIFICATION

2b GROUP

3 REPORT TITLE

INTERNAL WAVES IN THE ARCTIC OCEAN

4 DESCRIPTIVE NOTES *(Type of report and inclusive dates)*
Technical report.

5 AUTHOR(S) *(Last name, first name, initial)*

Yearsley, John Ross

6 REPORT DATE
September 1966

7a TOTAL NO. OF PAGES
63

7b. NO OF REFS
18

8a CONTRACT OR GRANT NO.
Nonr 266 (82)

b. PROJECT NO
Project Vela - Advanced Research Projects Agency

c

d

9a ORIGINATOR'S REPORT NUMBER(S)

CU-5-66 - Technical Report No. 5

9b. OTHER REPORT NO(S) *(Any other numbers that may be assigned this report)*

10 AVAILABILITY/LIMITATION NOTICES

Distribution of this document is unlimited

11 SUPPLEMENTARY NOTES

12 SPONSORING MILITARY ACTIVITY
Office of Naval Research
Department of the Navy
Washington, D. C.

13 ABSTRACT

A theoretical investigation is made of free internal gravity waves in a rotating fluid. An exponential density profile similar to that of the Canada Basin of the Arctic Ocean is used. The dispersion relation and eigenfunctions of the vertical amplitude are calculated.

An experimental investigation of temperature fluctuations at 60 and 125 meters was conducted at T-3 in the Arctic Ocean. Power spectra of the records show a rapid decrease of power with increasing frequency.

DD FORM 1 JAN 64 1473

Unclassified

Security Classification

14 KEY WORDS	LINK A		LINK B		LINK C	
	ROLE	WT	ROLE	WT	ROLE	WT
Internal waves Arctic Ocean Physical Oceanography Stratified fluids						

INSTRUCTIONS

1. ORIGINATING ACTIVITY: Enter the name and address of the contractor, subcontractor, grantee, Department of Defense activity or other organization *(corporate author)* issuing the report.

2*a*. REPORT SECURITY CLASSIFICATION: Enter the overall security classification of the report. Indicate whether "Restricted Data" is included. Marking is to be in accordance with appropriate security regulations.

2*b*. GROUP: Automatic downgrading is specified in DoD Directive 5200.10 and Armed Forces Industrial Manual. Enter the group number. Also, when applicable, show that optional markings have been used for Group 3 and Group 4 as authorized.

3. REPORT TITLE: Enter the complete report title in all capital letters. Titles in all cases should be unclassified. If a meaningful title cannot be selected without classification, show title classification in all capitals in parenthesis immediately following the title.

4. DESCRIPTIVE NOTES: If appropriate, enter the type of report, e.g., interim, progress, summary, annual, or final. Give the inclusive dates when a specific reporting period is covered.

5. AUTHOR(S): Enter the name(s) of author(s) as shown on or in the report. Enter last name, first name, middle initial. If military, show rank and branch of service. The name of the principal author is an absolute minimum requirement.

6. REPORT DATE: Enter the date of the report as day, month, year; or month, year. If more than one date appears on the report, use date of publication.

7*a*. TOTAL NUMBER OF PAGES: The total page count should follow normal pagination procedures, i.e., enter the number of pages containing information.

7*b*. NUMBER OF REFERENCES: Enter the total number of references cited in the report.

8*a*. CONTRACT OR GRANT NUMBER: If appropriate, enter the applicable number of the contract or grant under which the report was written.

8*b*, 8*c*, & 8*d*. PROJECT NUMBER: Enter the appropriate military department identification, such as project number, subproject number, system numbers, task number, etc.

9*a*. ORIGINATOR'S REPORT NUMBER(S): Enter the official report number by which the document will be identified and controlled by the originating activity. This number must be unique to this report.

9*b*. OTHER REPORT NUMBER(S): If the report has been assigned any other report numbers *(either by the originator or by the sponsor)*, also enter this number(s).

10. AVAILABILITY/LIMITATION NOTICES: Enter any limitations on further dissemination of the report, other than those imposed by security classification, using standard statements such as:

(1) "Qualified requesters may obtain copies of this report from DDC."

(2) "Foreign announcement and dissemination of this report by DDC is not authorized."

(3) "U. S. Government agencies may obtain copies of this report directly from DDC. Other qualified DDC users shall request through

_____."

(4) "U. S. military agencies may obtain copies of this report directly from DDC. Other qualified users shall request through

_____."

(5) "All distribution of this report is controlled. Qualified DDC users shall request through

_____."

If the report has been furnished to the Office of Technical Services, Department of Commerce, for sale to the public, indicate this fact and enter the price, if known.

11. SUPPLEMENTARY NOTES: Use for additional explanatory notes.

12. SPONSORING MILITARY ACTIVITY: Enter the name of the departmental project office or laboratory sponsoring *(paying for)* the research and development. Include address.

13 ABSTRACT: Enter an abstract giving a brief and factual summary of the document indicative of the report, even though it may also appear elsewhere in the body of the technical report. If additional space is required, a continuation sheet shall be attached.

It is highly desirable that the abstract of classified reports be unclassified. Each paragraph of the abstract shall end with an indication of the military security classification of the information in the paragraph, represented as *(TS)*. *(S)*. *(C)*, or *(U)*

There is no limitation on the length of the abstract. However, the suggested length is from 150 to 225 words.

14. KEY WORDS: Key words are technically meaningful terms or short phrases that characterize a report and may be used as index entries for cataloging the report. Key words must be selected so that no security classification is required. Identifiers, such as equipment model designation, trade name, military project code name, geographic location, may be used as key words but will be followed by an indication of technical context. The assignment of links, rules, and weights is optional.